Design of a Radial Mode Piezoelectric Transformer for a Charge Pump Electronic Ballast with High Power Factor and Zero Voltage Switching

by

Weixing Huang

Thesis submitted to the faculty of the
Virginia Polytechnic Institute and State University
in partial fulfillment of the requirements for the degree of

Master of Science
in
Electrical Engineering

APPROVED

_____

Dan Y. Chen, Chairman

_____ _____

Alex Q. Huang Douglas K. Lindner

April 21, 2003
Blacksburg, Virginia

Key words: Piezoelectric Transformer, PFC, Electronic Ballast

Design of a Radial Mode Piezoelectric Transformer for a Charge Pump Electronic Ballast with High Power Factor and Zero Voltage Switching

by

Weixing Huang

Dr. Dan Y. Chen, Chairman

Electrical Engineering

(ABSTRACT)

In a conventional electronic ballast for a fluorescent lamp, inductor-capacitor-transformer tank circuit is used. A Piezoelectric Transformer (PT) can potentially be used to replace such a tank circuit to save space and cost. In the past, ballast design using a PT requires selecting a PT from available samples which are normally not matched to specific application and therefore resulting in poor performance. In this thesis, a design procedure was proposed for designing a PT tailored for a 120-V 32-W electronic ballast with high power factor, high efficiency and Zero-Voltage-Switching (ZVS) of the inverter transistors that drive the lamp. This involves selection of PT materials, determination of geometries and the number of physical layers of the PT. A radial mode piezoelectric transformer prototype based on this design process was fabricated by Face Electronics Inc. and was tested experimentally, the results showed that the ballast using this custom-made PT achieved high power factor, Zero-Voltage-Switching and a 83% overall efficiency.

Acknowledgments

I would like to express my sincerest appreciation to my research and academic advisor, Dr. Dan Y. Chen, for his invaluable guidance, encouragement, and continue support throughout my graduate study and research in Virginia Tech.

I am grateful to the other two members of my advisory committee, Dr. Alex Q. Huang and Dr. Douglas K. Lindner for their support, suggestion and encouragement.

I would like to thank my project partners, Mr. Eric M. Baker, Mr. Jinghai Zhou, Dr. Fengfeng Tao, Dr. Weiping Zhang for their great help and valuable suggestions in the piezoelectric transformer project team.

It has been a great pleasure to associate with the incredible faculty, staff and student at the Center for Power Electronics System (CPES). I would like to thank Dr. Fred C. Lee, Dr. Dushan Boroyevich, Dr. Dann van Wyk and Dr. Jason Lai for their wonderful graduate courses on power electronics that will be exceptionally helpful for my future career. I would like to thank Mr. Robert Martin, Mr. Steve Chen, Ms. Elizabeth Tranter, Ms Trish Rose and all other CPES staff for their assistance and kindness. I also would like to thank all my friends in CPES for their help during my study here, especially Mr. Liyu Yang for taking pictures for the PT samples, I will cherish the friendship that I have made here.

I would like to present my heartfelt appreciation to my beloved wife, Yihui, for her endless love, understanding and support and wish her success for her study and research in MIT. Thanks also extend to my parents, my brother, my sister and all other family members for their love and their support.

Special thanks to my host family, Mr. Tom Wieboldt, Ms. Ali Wieboldt and Miss Elsa Wieboldt. All the wonderful time that we spent together is still vivid in my mind.

Thank you all, for the influence that you have made on my life.

Table of Contents

List of Illustrations

List of Tables

CHAPTER 1 INTRODUCTION

1.1 Background

In the past years, the idea of smart material has been interesting to the researchers and engineers as a new category of physical material that has integrated sensor, actuator, power electronics and microprocessor [1]. Among all the smart materials, piezoelectric and electrostrictive materials are considered to especially promising due to their unique physical properties such as higher accuracy, higher response speed, lower power requirements etc., compared to other materials. As a result, actuator, transducer, and sensor made from of these two materials have been widely used in piezoelectric transformers, which will be discussed in this thesis and many other applications such as ultrasonic motors, deformable mirrors, active vibration cancellation, mechanical micropositioners etc.

Due to the tide of miniaturization and integration of modern power electronics system, in which the magnetic components remain as the bulkiest and costliest components, many efforts have been taken on piezoelectric transformer as an alternative to the magnetic transformer in recent years. Over the conventional magnetic transformer, piezoelectric transformer has several inherit advantages: nonflammability, small size, low profile, low cost, low EMI, no winding, high degree of insulation, high efficiency, high power density, high operation frequency and suitability for automated manufacturing. Moreover, they are especially attractive for low power, high voltage application where making and testing the high voltage transformer is laborious. However, drawback such as mounting, packaging, temperature effect and thermal issue are also need to be considered.

While piezoelectric transformers were developed in the late 1950s [2, 3], their application was limited because of the immature materials fabrication technology, poor material and mechanical reliability and lack of circuit driving techniques. With the improvement in material and fabrication technology, piezoelectric transformer has been used in a lot of applications in recent years, such as, electronic ballast for fluorescent

lamps and inverter for backlighting the LCDs in a notebook computer [4-15], AC adapter for mobile computer [16], battery charger for mobile phones [17], gate drivers of MOSFET and IGBTs [18] and signal isolation [19], DC/DC converter [20-25], photomultiplier high voltage power supply [26-28], electronic ignition system [29], clock pulse shaping circuit [30], and driving circuit for piezoelectric actuators such as ultrasonic motors[31-33]. It was even used as a discharge exciter for light emission [34-35].

1.2 Review of Piezoelectric Transformer

In a conventional magnetic transformer, the electrical input is converted to magnetic energy and then reconverted the magnetic energy back to an electrical output. The piezoelectric transformer has an analogous operating mechanism. It converts an electrical input into mechanical energy and subsequently reconverts the mechanical energy back to an electrical output.

Piezoelectric transformer is a combination of piezoelectric actuator and transducer, which serve as the primary side and the secondary side respectively. Both the piezoelectric actuator and piezoelectric transducer are made of piezoelectric materials. First discovered in 1880 [36], most piezoelectric materials can be categorized into one of the following three classes: Single crystals such as Quartz, polymers such as polyvinylidine fluoride (PVDF) and poled ceramics such as PZT, or Pb(Zr,Ti)O3. Within these three categories of piezoelectric materials, PZT material represents the largest portion of the commercial market due to its high coupling coefficients and its versatility with regard to chemical substitutions. It is referred as piezocermic in this thesis. The characterization of piezoceramics was summarized in [37]. Generally speaking, the two piezoelectric elements, piezoelectric actuator and the piezoelectric transducer, can work in either longitudinal mode or transverse mode with a corresponding resonant frequency.

According to the different vibration mode and mechanical structures, the piezoelectric transformers could be classified to three main categories [38]: Rosen-Type, thickness vibration mode and radial vibration mode.

A) Rosen-type PT

The Rosen-type piezoelectric transformer [39-41] is a combination of transverse mode piezoelectric actuator and longitudinal mode piezoelectric transducer as shown in Fig. 1.1. Referring to this figure, the actuator converts V_{in} into mechanical vibration which couples the transducer, which in turn converts mechanical vibration to V_{out}. Because of the inherent high voltage gain associated with the Rosen-type piezoelectric transformers, while matching high-impedance resistive load (around 100k) with optimal efficiency, they often are referred to as high-voltage piezoelectric transformers which are suitable for driving high-voltage lamps, such as cold cathode fluorescent lamps, used as the back-light source for flat panel displays of notebook computers.

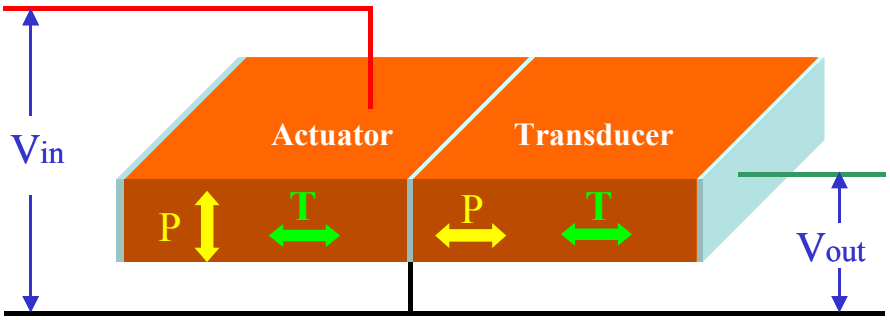

(P: polarization, T: stress)

Fig. 1.1. Rosen-type piezoelectric transformer

B) Thickness Vibration Mode PT

The thickness vibration mode piezoelectric transformer [42-45] is a combination of longitudinal mode piezoelectric actuator and longitudinal mode piezoelectric transducer, as shown in Fig. 1.2. The thickness vibration mode piezoelectric transformer is also known as a low-voltage piezoelectric transformer because of its inherent low voltage gain, while matching a low impedance resistive load (around 10 Ohm) with

optimal efficiency. Its present applications include DC/DC power converter and adapter applications.

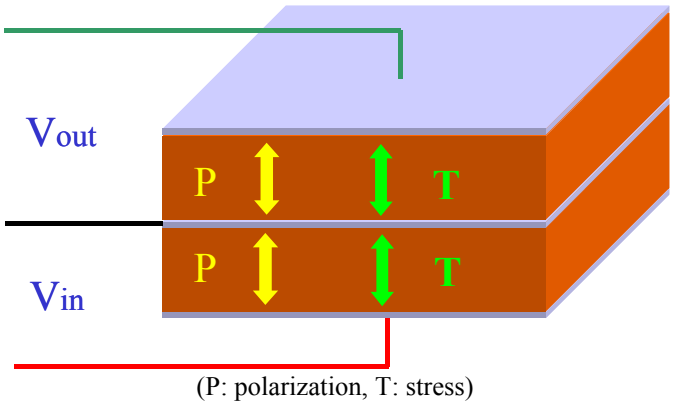

Fig. 1.2. Thickness vibration mode piezoelectric transformer

C) Radial Vibration Mode PT

The radial vibration mode piezoelectric transformer [38, 46-55] is a combination of piezoelectric actuator and transducer that both operate in the transverse mode, as shown in Figure 1.3.

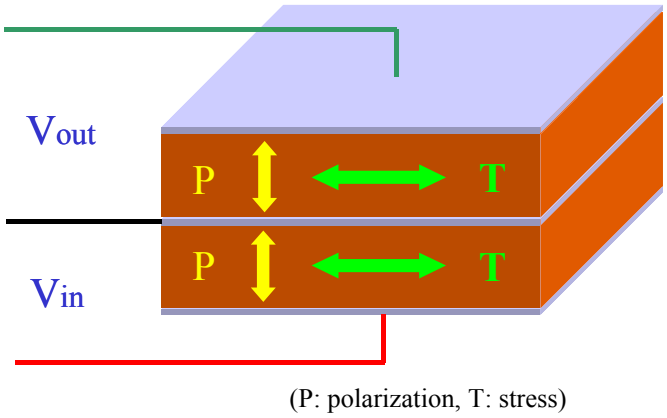

Fig. 1.3. Radial vibration mode piezoelectric transformer

Besides these three main categories of piezoelectric transformer, piezoelectric transformers with some other special structures were also introduced in recent publications [56-59]. Compared to each other, these piezoelectric transformers have their own advantages but also disadvantage so as to be suitable for some special applications. Changing the composition of the piezocermic materials, which was used to make the

piezoelectric transformer so as to improve the performance of the piezoelectric transformer, was also reported in recent publications [33, 60].

In order to increase the step-up or step-down ratio, either the electric actuator or electrical transducer can be made up of more than one layer of piezocermic materials. This kind of piezoelectric transformer was called multiplayer piezoelectric transformer, as report in many papers [61-65].

1.3 Thesis Objective and Outline

The objectives of this thesis research are as follow:

1) Establish clear relationships between the ballast circuit performance parameters and the PT device parameters. To do this, an intermediate link of PT electrical equivalent circuit is necessary. The relationships are depicted in the following diagram.

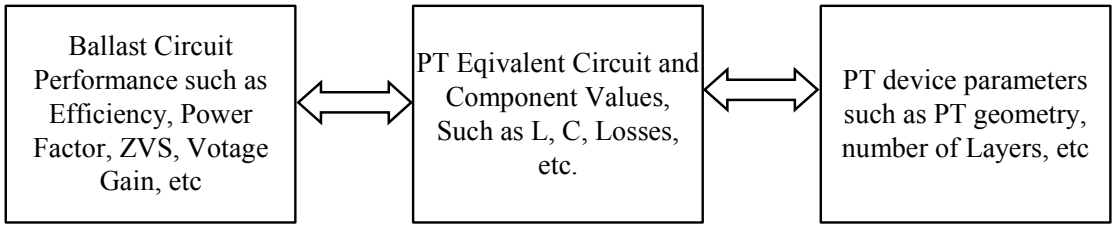

2) Propose a design step to design a PT for a given ballast performance specifications. A practical 120-V, 32-W ballast with high efficiency, high power factor and Zero-Voltage-Switching (ZVS) is taken as an example to illustrate such design procedure. Radial mode PT is considered because up to this point, only radial mode PT capable of such power handling capability has been reported.

3) Fabricate a PT based on objective 2 above and test the prototype in a practical charge-pump ballast circuit.

There are four chapters in this thesis.

Chapter 2 Reviews and summarizes the characterization of the radial mode piezoelectric transformer, including the theory of operation, equivalent circuit, relationship between the equivalent circuit parameters and physical dimensional

parameters. Design method and procedure presented in chapter 3 will be based on the results in this chapter.

Chapter 3 presents the design method for radial mode piezoelectric transformer used in PFC electronic ballast application. A step-by-step design procedure for the PT proposed for a 32-W 120-V electronic ballast application. Complicated relationships between the circuit performance parameters and the PT parameters were developed and used to reach a workable solution. A custom-designed PT was fabricated and tested.

Chapter 4 gives the conclusion of the work and recommendation for future works.

The references list the reference materials collected for this project. The appendix includes two MATHCAD programming files, one is used to design the radial mode piezoelectric transformer and the other one is used to analysis the performance of the radial mode piezoelectric transformer.

CHAPTER 2 OVERVIEW OF THE RADIAL MODE PIEZOELECTRIC TRRANSFORMERS

2.1 Introduction

In chapter 1, a square-shape radial vibration mode piezoelectric transformer was introduced, as shown in Fig. 1.3. Because for this kind of radial vibration mode piezoelectric transformer the distances from the center to the edge of the electrode plates are not the same, its wavelengths of the planar vibration are not the same, which causes additional vibration frequencies. In order to eliminate the additional vibration frequencies other than the fundamental vibration frequency, Face Electronics Inc. proposed a practical radial vibration mode piezoelectric transformer, which is made in a round shape. In Fig. 2.1, the round-shape radial vibration mode piezoelectric transformer or Transoner® has the same distance, r, from the center to the edge on the electrode plates. Therefore, the fundamental vibration wavelength, λ of the round-shape radial vibration mode piezoelectric transformer is

$$\lambda = 2 \cdot r \tag{2.1}$$

where r is the radius of round-shape radial vibration mode piezoelectric transformer.

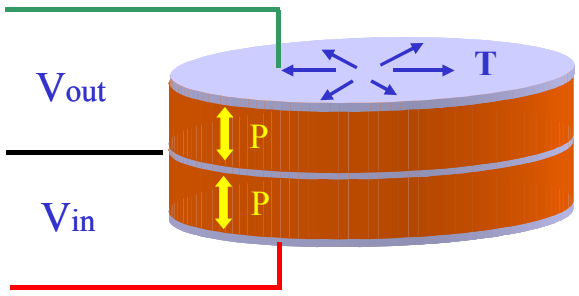

(P: polarization, T: stress)

Fig. 2.1. Round shape radial vibration mode piezoelectric transformer

More specifically, the Transoner is constructed by using an adhesive to bond the copper electrodes to circular piezoceramic disks, as shown in Fig. 2.2.

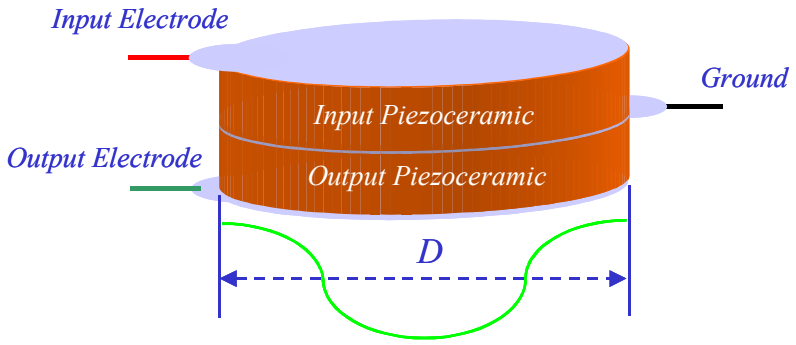

Fig. 2.2. Construction of Transoner

For the Transoner, the fundamental vibration frequency is inversely proportional to the radius and directly proportional to the wave propagation speed of the material. [46] as shown in (2.2)

$$f_r = \frac{N_R}{D} \tag{2.2}$$

Where: D is the diameter and N_R is the material wave speed.

2.2 Equivalent Circuit Models and Characteristic Equations

The equivalent circuit Models and characteristic equations of the Transoner have been carefully derived in [38] and are summarized here. The conventional simplified equivalent circuit for the Transoner was shown in Fig. 2.3

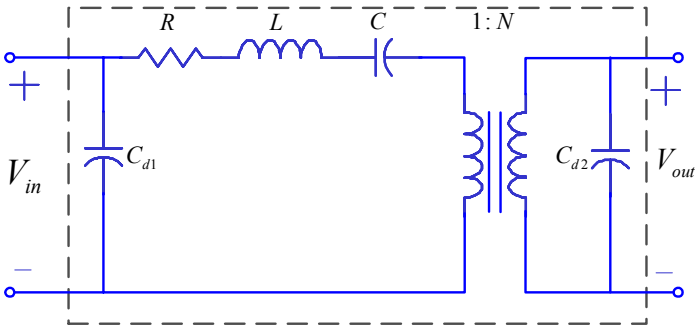

Fig. 2.3. Simplified conventional equivalent circuit of Transoner

The component value of the equivalent circuit in Fig. 2.3 are related to physical parameters of the PT. Equations (2.3~2.8) show such relationships:

$$C_{d1} = \frac{N_1 \cdot \pi \cdot r^2 \cdot \varepsilon_{33}^T \cdot \left(1 - \frac{{d_{31}}^2}{\varepsilon_{33}^T \cdot S_{11}^E}\right)}{t_1} \tag{2.3}$$

$$R = \frac{\sqrt{2 \cdot \rho \cdot S_{11}^{E^3}} \cdot (N_1 \cdot t_1 + N_2 \cdot t_2)}{16 \cdot r \cdot Q_m \cdot (N_1 \cdot d_{31})^2} \tag{2.4}$$

$$L = \frac{\rho \cdot S_{11}^{E^2} \cdot (N_1 \cdot t_1 + N_2 \cdot t_2)}{8 \cdot \pi \cdot (N_1 \cdot d_{31})^2} \tag{2.5}$$

$$C = \frac{16 \cdot r^2 \cdot (d_{31} \cdot N_1)^2}{\pi \cdot S_{11}^E \cdot (N_1 \cdot t_1 + N_2 \cdot t_2)} \tag{2.6}$$

$$C_{d2} = \frac{N_2 \cdot \pi \cdot r^2 \cdot \varepsilon_{33}^T \cdot \left(1 - \frac{{d_{31}}^2}{\varepsilon_{33}^T \cdot S_{11}^E}\right)}{t_2} \tag{2.7}$$

$$N = \frac{N_1}{N_2} \tag{2.8}$$

Definitions of the material symbols in the above equation are summarized in Table 2.1.

TABLE 2.1 MATERIAL SYMBOLS AND DEFINITIONS

ρ	Density
ε^T_{33}	Permittivity
Q_m	Mechanical Quality Factor
d_{31}	Piezoelectric Coefficient
S^E_{11}	Elastic Compliance
$\tan\delta$	Dissipation Factor
N_R	Radial Mode Frequency Constant
t_1	Primary Layer Thickness
t_2	Secondary Layer Thickness
N_1	Number of Primary Layers
N_2	Number of Secondary Layers
r	Radius of the Layers

In Fig. 2.3, the internal resistance R stands for the mechanical loss of the piezoelectric device. To consider the dielectric loss of the material for better efficiency predication, two frequency dependent resistors, R_{cd1} and R_{cd2} can be added in parallel with the input and output capacitances, C_{d1} and C_{d2} respectively, as shown Fig 2.4. Moreover, the ESR or equivalent series resistance of the capacitor can also be considered for better accuracy. Modeling and measurement of the mechanical and dielectric loss were discussed in [66-70].

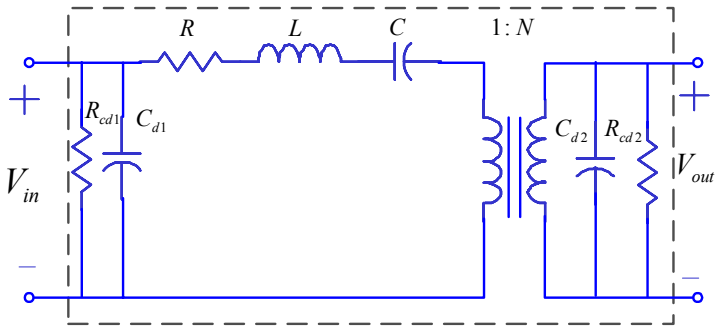

Fig. 2.4. Conventional equivalent circuit of Transoner

In Fig 2.4, R_{cd1} and R_{cd2} could be estimated by [72].

$$R_{cd1} = \frac{1}{\omega_s \cdot C_{d1} \cdot \tan\delta} \tag{2.9}$$

$$R_{cd2} = \frac{1}{\omega_s \cdot C_{d2} \cdot \tan\delta} \tag{2.10}$$

Besides the major vibration mode, there are many spurious vibration modes that exist in the piezoelectric transformers. A multi-branch equivalent circuit was proposed in [38] to describe other spurious vibration mode adjacent to the major vibration mode and match the measured voltage gain, as shown in Fig. 2.5. However, the piezoelectric electric transformer is normally driven around the major vibration frequency to achieve high efficiency. For this reason, only the equivalent circuit of the Transoner shown in Fig. 2.4 will be used in this thesis.

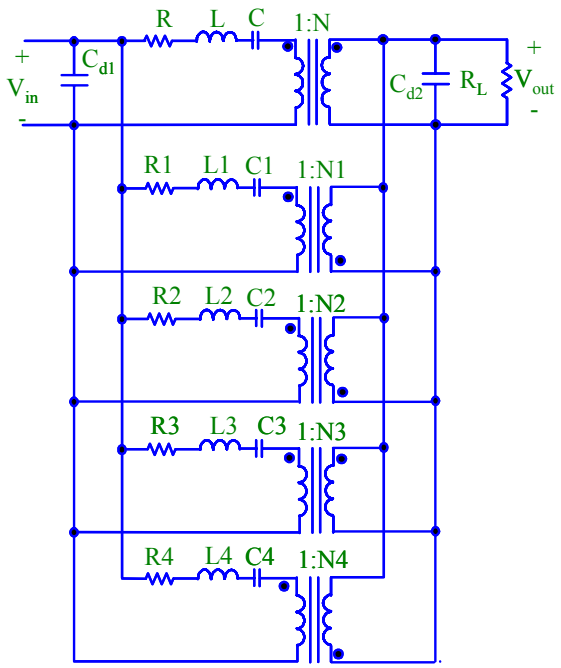

Fig. 2.5. Multi-branch equivalent circuit of Transoner

2.3 Equivalent Circuit Parameters Measurement using Y-Parameter Model

Generally speaking, the equivalent circuit parameters of the piezoelectric transformer can be measured by HP4195A impedance analyzer. HP4195A impedance analyzer provides an admittance equivalent circuit model or Y-Parameter model, which is identical to the simplified conventional equivalent of the Transoner with the input or output terminal shorted, as shown in Fig. 2.6. Based on this, the equivalent circuit parameters of the Transoner can be measured around the resonant frequency. Detailed measurement procedure can be found in [38].

According to equations (2.3~2.8), the equivalent circuit parameters could also be calculated from the physical dimensional parameters: N_1, N_2, t_1, t_2 and r. [38] showed that parameters calculated from the above equation are quite close to the parameters measured by the HP4195A, which verified the accuracy of the equivalent circuit in Fig. 2.1.

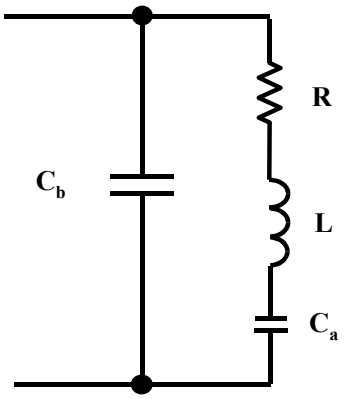

Fig. 2.6. Y-parameter equivalent circuit model provided by HP4195A

2.4 Performance Analysis of the Radial Mode Piezoelectric Transformer

Using the equivalent circuit, PT characteristics such as input impedance, voltage gain, efficiency and optimal load can be analyzed with a given load. A MATHCAD program was developed for this purpose and is provided in appendix I.

A. Optimal Load at given frequency

For a given frequency ω, there is an optimal load which gives the maximum efficiency of the PT. In Fig. 2.3, connecting a resister load R_L in parallel with the output capacitance C_{d2} and reflecting the secondary side to the primary side, the equivalent circuit becomes Fig. 2.7. In the circuit, N is the turns ratio of the piezoelectric transformer and is defined as (2.8).

For the given frequency ω, the parallel connected R_L and C_{d2} can be transformed to be series connected, as shown in Fig. 2.8.

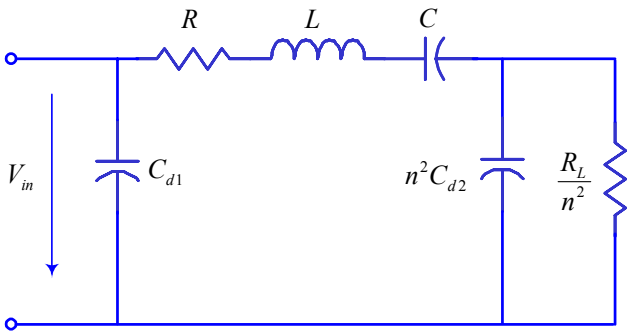

Fig. 2.7. PT equivalent circuit with secondary side reflecting to the primary side

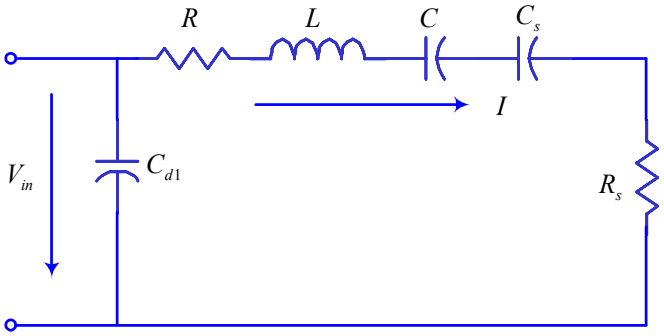

Fig. 2.8. PT equivalent circuit with transforming the parallel connection to series connection.

In Fig. 2.8, the equation governing R_s and C_s are shown in (2.11) and (2.12)

$$R_s = \frac{R_L}{n^2} \cdot \frac{1}{1+(\omega \cdot C_{d2} \cdot R_L)^2} \tag{2.11}$$

$$C_s = n^2 \cdot C_{d2} \cdot \frac{1+(\omega \cdot C_{d2} \cdot R_L)^2}{(\omega \cdot C_{d2} \cdot R_L)^2} \tag{2.12}$$

then efficiency of the circuit could be expressed by (2.13)

$$\eta = \frac{P_o}{P_{in}} = \frac{I_{rms}^2 \cdot R_s}{I_{rms}^2 \cdot R_s + I_{rms}^2 \cdot R} = \frac{R_s}{R_s + R} = \frac{1}{1+\frac{R}{R_s}}$$
$$= \frac{1}{1+\left[1+(\omega \cdot C_{d2} \cdot R_L)^2\right] \cdot \frac{n^2 \cdot R}{R_L}} \tag{2.13}$$

Take

$$\frac{d\eta}{dR_L} = 0$$

then

$$\eta_{\max} = \frac{R_{L(OPT)}}{2n^2 R + R_{L(OPT)}} \tag{2.14}$$

where

$$R_{L(OPT)} = \frac{1}{\omega \cdot C_{d2}} \tag{2.15}$$

Equation (2.14) and (2.15) showed that for a given driving frequency, the maximum efficiency of the PT is obtained when the load is equal to the impedance of the output capacitor. This characteristic will be used later in PT design procedure given in chapter 3.

B. Resonance frequency at given load.

For a given load R_L, there is also a resonance frequency which gives the maximum voltage gain of the PT.

For Fig. 2.7, when the output is shorted (R_L=0), the resonant frequency of the circuit is

$$f_{SC} = \frac{1}{2\pi\sqrt{L \cdot C}} \tag{2.16}$$

When the output is open (RL=∞), the resonant frequency of the circuit of the circuit is

$$f_{OC} = \frac{1}{2\pi\sqrt{L \cdot (C // n^2 C_{d2})}} = f_{SC} \cdot \sqrt{1 + \frac{C}{n^2 C_{d2}}} \tag{2.17}$$

When a finite load resistance R_L is given, resonant frequency f_r is:

$$f_r = \frac{1}{2\pi\sqrt{L \cdot \frac{C \cdot C_s}{C + C_s}}} \tag{2.18}$$

where C_s is

$$C_s = n^2 \cdot C_{d2} \cdot \frac{1+(2\pi f_r \cdot C_{d2} \cdot R_L)^2}{(2\pi f_r \cdot C_{d2} \cdot R_L)^2} \tag{2.19}$$

solve f_r from (2.19), yield:

$$f_r = \frac{\sqrt{2 \cdot L \cdot C \cdot \left(-L \cdot C \cdot N^2 + N^2 \cdot {C_{d2}}^2 \cdot {R_L}^2 + C_{d2} \cdot {R_L}^2 \cdot C + \sqrt{\Delta}\right)}}{4 \cdot \pi \cdot L \cdot C \cdot N \cdot C_{d2} \cdot R_L} \tag{2.20}$$

where

$$\begin{aligned}\Delta = {} & L^2 \cdot C^2 \cdot N^4 + 2 \cdot L \cdot C \cdot N^4 \cdot {C_{d2}}^2 \cdot {R_L}^2 - 2 \cdot L \cdot C^2 \cdot N^2 \cdot C_{d2} \cdot {R_L}^2 \\ & + N^4 \cdot {C_{d2}}^2 \cdot {R_L}^4 + 2 \cdot {C_{d2}}^3 \cdot {R_L}^4 \cdot C \cdot N^2 + {C_{d2}}^2 \cdot {R_L}^4 \cdot C^2\end{aligned} \tag{2.21}$$

(2.20) showed that for a given load R_L, there is a corresponding resonant frequency f_r of the circuit and it should be between f_{sc} and f_{oc}.

C. Voltage Gain, Output Power and Efficiency at resonance

For a given load R_L, if the piezoelectric transformer is driven at the resonant frequency f_r that is corresponding to the given R_L, the voltage gain, output power and efficiency at resonance can be expressed by (2.22)-(2.24) respectively.

$$A_v = 20 \cdot \log\left(\frac{R_L \cdot \sqrt{1+(2 \cdot \pi \cdot f_r \cdot C_{d2} \cdot R_L)^2}}{n^2 \cdot R \cdot \left[1+(2 \cdot \pi \cdot f_r \cdot C_{d2} \cdot R_L)^2\right] + R_L}\right) \tag{2.22}$$

$$P_o = \frac{{V_{in}}^2 \cdot n^2 \cdot R_L \cdot \left[1+(2 \cdot \pi \cdot f_r \cdot C_{d2} \cdot R_L)^2\right]}{\left[n^2 \cdot R \cdot \left[1+(2 \cdot \pi \cdot f_r \cdot C_{d2} \cdot R_L)^2\right] + R_L\right]^2} \tag{2.23}$$

$$\eta = \frac{1}{1+\left[1+(2 \cdot \pi \cdot f_r \cdot C_{d2} \cdot R_L)^2\right] \cdot \frac{n^2 \cdot R}{R_L}} \tag{2.24}$$

Example:

Take sample AJ-1 as an example as shown in Fig. 2.9.

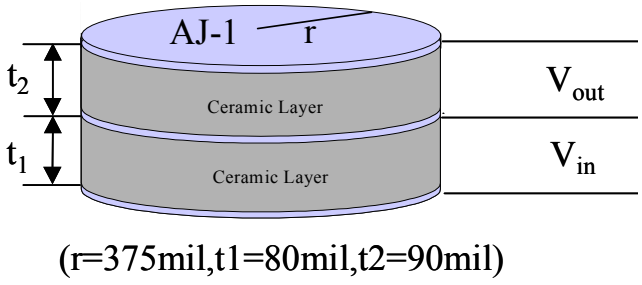

Fig. 2.9. PT sample AJ-1

The equivalent circuit parameters are as following:

R=11.18 Ohm, L=9.50mH, C=192.361pF, N=0.969466, C_{d1}=1.469nF, C_{d2}=1.347nF

According to (2.20~2.24), the characteristic curve of AJ-1 can be plotted as Fig. 2.10.

D. Normalized voltage gain curve

From the equivalent circuit of the piezoelectric transformer we can see it can be treated as series-parallel resonant converter. When analyzing the resonant converter, the voltage gain vs. the normalized frequency curve is very important [71], especially for the design of PT for DC/DC converter application.

In Fig. 2.7, Define

$$k=\frac{C'_{d2}}{C} \qquad \omega_0=\frac{1}{\sqrt{LC}} \qquad Z_0=\sqrt{\frac{L}{C}} \qquad Q_m=\frac{Z_0}{R} \qquad Q=\frac{Z_0}{R'_L}$$

It is easy to get

$$|A|=\frac{1}{\sqrt{\left\{1+\frac{Q}{Q_m}+k\left[1-\left(\frac{\omega}{\omega_0}\right)^2\right]\right\}^2+\left\{\frac{\omega}{\omega_0}\cdot\frac{k}{Q_m}+\frac{\omega_0}{\omega}\cdot Q\cdot\left[\left(\frac{\omega}{\omega_0}\right)^2-1\right]\right\}^2}} \tag{2.25}$$

Fig 2.11 shows the normalized voltage gain curve of AJ-1 when the load is 1, 10, 100, 1k, 10k, 100k, 1M Ohms respectively.

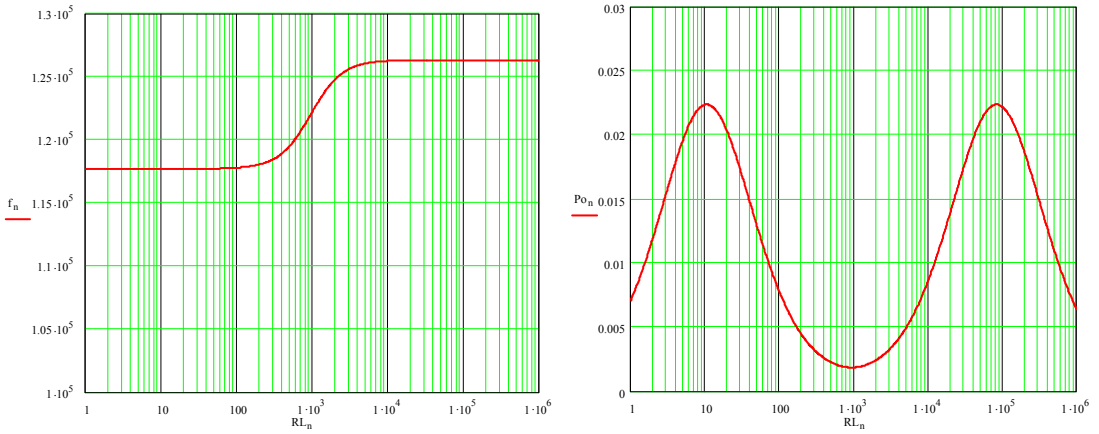

(a) Resonant frequency for given load (b) Normalized output power at resonance

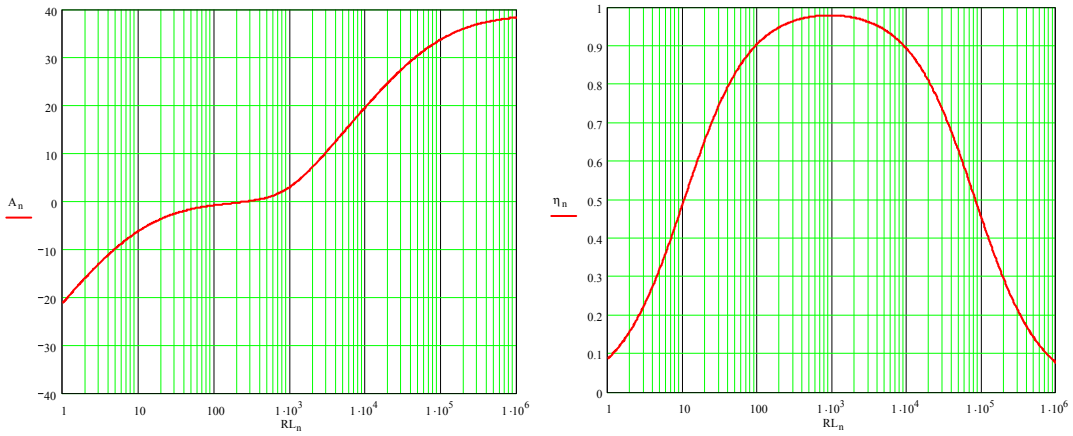

(c) Voltage gain at resonance (dB) (d) Efficiency at resonance

Fig. 2.10. Characteristic curves of AJ-1.

(a) Resonance frequency for given load; (b) Normalized output power at resonance;
(c) Voltage gain at resonance (dB); (d) Efficiency resonance.

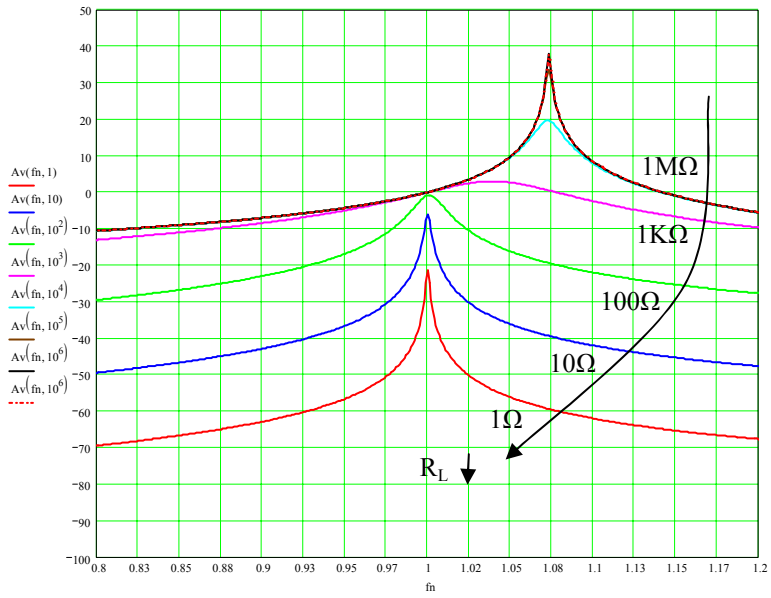

Fig. 2.11. Voltage gain Vs. normalized frequency at different load conditions

E. 3-D Analysis

From the above discussion, one can find that the voltage gain, output power and efficiency are functions of both the load resistance and the driving frequency of the circuit as shown in (2.26~2.30) without considering the dielectric loss. Similar equations can be obtained by using Fig 2.4 instead of Fig 2.3 if the dielectric loss needs to be considered. When the dielectric losses are considered, the analytical expressions for the voltage gain, output power and efficiency are more complicated. However, it is observed that the PT characteristics do not deviate much near the resonant frequency. In the actual design, one will use the characteristics of PT near the resonant frequency anyway. 3-D characteristic of the PT can be visualized by using the attached MATHCAD file. Take the 3-D efficiency plot of AJ-1 as an example, as shown in Fig 2.12(a)~(c). (a) shows the efficiency curve without considering the dielectric loss, (b) shows the efficiency plot including the dielectric loss. (c) shows the difference between the two efficiency curves.

$$A_V(R_L, f_s) = \left| N \cdot \frac{\left(N^2/R_L + j2\pi f_s N^2 C_{d2}\right)^{-1}}{R + j2\pi f_s L + 1/j2\pi f_s C + \left(N^2/R_L + j2\pi f_s N^2 C_{d2}\right)^{-1}} \right| \tag{2.26}$$

$$Z_{in}(R_L, f_s) = \frac{(j2\pi f_s C_{d1})^{-1} \cdot \left(R + j2\pi f_s L + 1/\, j2\pi f_s C + \left(N^2/R_L + j2\pi f_s N^2 C_{d2}\right)^{-1}\right)}{(j2\pi f_s C_{d1})^{-1} + \left(R + j2\pi f_s L + 1/\, j2\pi f_s C + \left(N^2/R_L + j2\pi f_s N^2 C_{d2}\right)^{-1}\right)} \tag{2.27}$$

$$P_{in}(R_L, f_s) = \mathrm{Re}\left(\frac{V_{in}^{\ 2}}{Z_{in}(R_L, f_s)}\right) \tag{2.28}$$

$$P_{out}(R_L, f_s) = \frac{\left(V_{in} \cdot A_V(R_L, f_s)\right)^2}{R_L} \tag{2.29}$$

$$\eta(R_L, f_s) = \frac{P_{out}(R_L, f_s)}{P_{in}(R_L, f_s)} \tag{2.30}$$

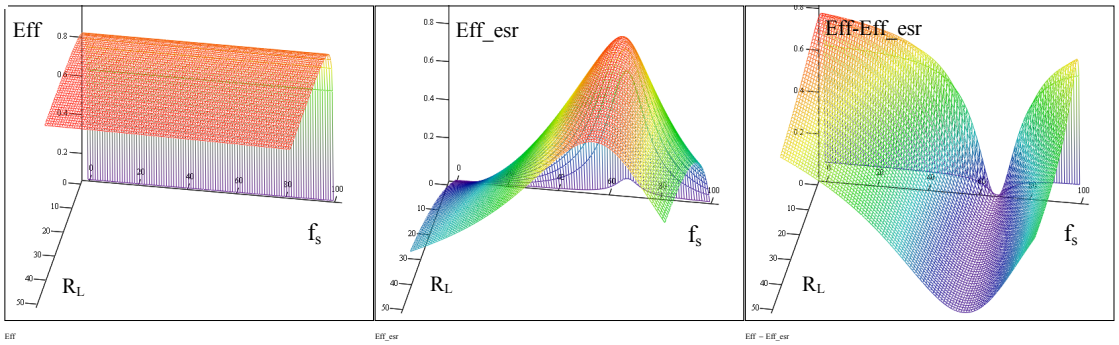

(a) (b) (c)

Fig. 2.12. 3-D plot of the characteristics of the PT AJ-1

(a) Efficiency without considering the dielectric loss; (b) Efficiency with considering the dielectric loss; (c) The difference between the efficiency with and without considering the dielectric loss

CHAPTER 3 RADIAL MODE PIEZOELECTRIC TRANSFORMER DESIGN FOR PFC BALLAST

3.1 Introduction

Applications of piezoelectric transformers (PT) to lamp ballast circuits have been reported in recent years [4-12]. It has been reported that a longitudinal vibration-mode (or Rosen-type) PT was used to power Cold-Cathode Fluorescent Lamps (CCFL) for notebook computer backlight display applications [72]. In this application, a high step-up voltage ratio (in the range of 100) and relatively low power (5 watt range) are required. Recently, the usage of a radial-mode PT for powering a conventional 32-watt fluorescent lamp from line power was reported [4, 5]. In this application, the requirement on voltage gain is low but the output power is in the range of 32 watts.

In the past, PTs used in such applications have been selected from available samples, which may not match the application. It's a well-known fact that for an unmatched load condition, the efficiency of a PT can be very poor as shown by Fig. 2.10 (d). Recently, it has been reported that a radial-mode PT has been custom designed for a 120-V, 32-watt fluorescent lamp ballast application using a standard half-bridge inverter [46, 73].

In this chapter, the focus is on the design of a PT custom made for a charge pump ballast circuit for a 120-V, 32-watt fluorescent lamp. Besides providing proper lamp starting voltage and steady-state voltage gain, the ballast circuit also has to be such that the main inverter circuit must have zero-voltage-switching (ZVS) operation, and have nearly unit power factor. And all of these requirements can be accomplished by properly designing a proper PT to replace the tank circuit conventionally consisting of inductor and capacitors. In the end, minimum components are used and both the efficiency and the power factor performance are excellent.

In the chapter, a brief review of the charge pump circuit will be described first in section 3.2, followed by a description of the PT equivalent circuit in section 3.3. Then a design procedure of the PT will be presented in section 3.4. Prototype PTs based on the proposed design procedure were then fabricated by FACE Electronics Inc. and tested in the circuit measurement. The experimental results will be shown in section 3.5.

3.2 Charge Pump Electronic Ballast Circuit

Fig. 3.1 shows a conventional electronic ballast with a complicated inductor-capacitor-transformer tank. A piezoelectric transformer can be used to replace the entire tank to save cost and reduce the complexity of the circuit. A PT-based current source charge-pump PFC electronic ballast circuit was proposed in [4] recently, as shown in Fig. 3.2. In this current source charge pump circuit, the input capacitor of the PT, C_{d1}, was utilized as the turn-off snubber of the circuit switch and part of the charge pump capacitor. Compared to the non-PFC ballast developed by Lin [50], only one capacitor and two diodes are added to achieve PFC function. The key waveforms of the circuit are shown in Fig. 3.3. Operation principle of this circuit was analyzed in detail in [4]. More information about charge pump power factor correction can be found in [74].

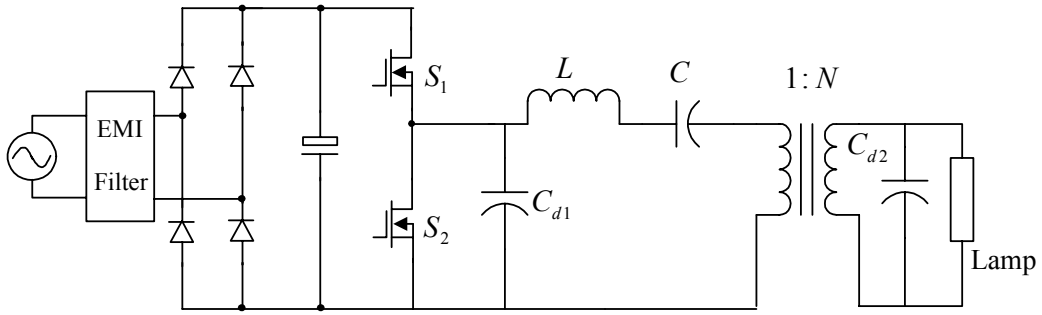

Fig. 3.1. Conventional electronic ballast with a complicated resonant tank

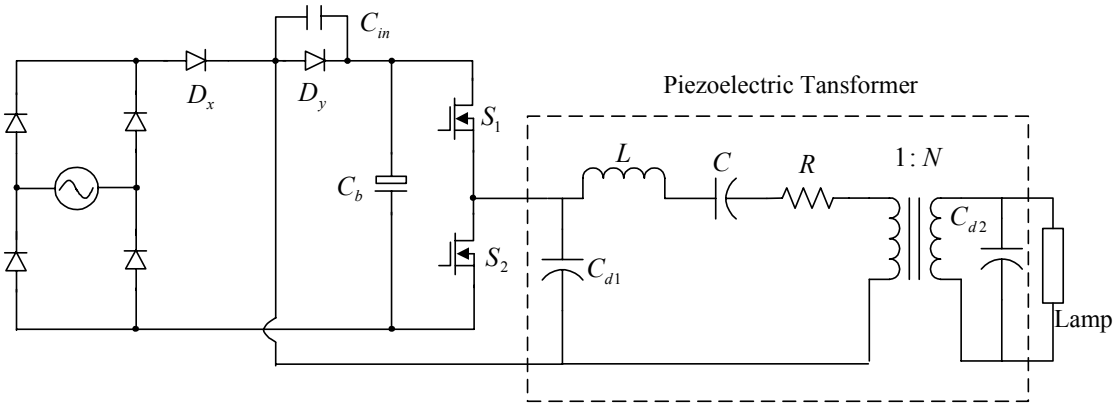

Fig. 3.2. The PT-based current source charge pump PFC electronic ballast

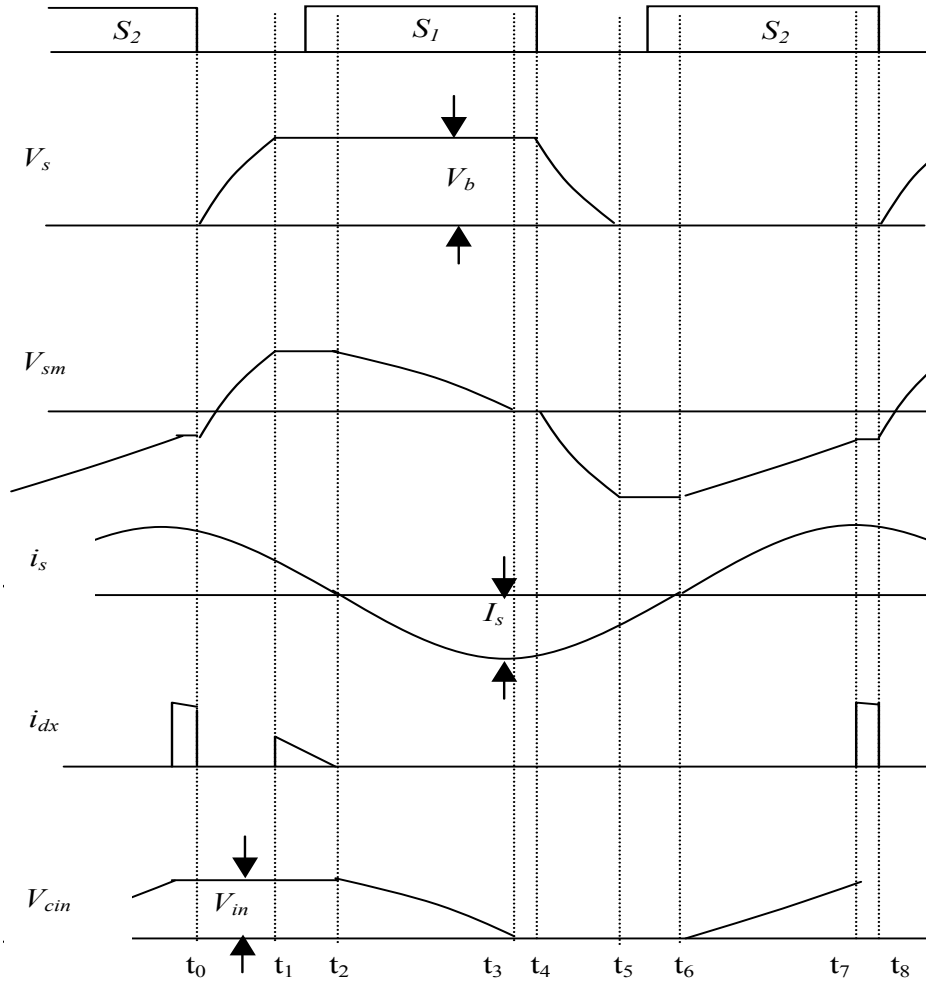

Fig. 3.3. Switching waveforms of the PT-based charge pump electronic ballast

3.3 PT Equivalent Circuit and Parameters Equations

As we summarized in Chapter 2, Figure 3.4 shows the structure of a 2-layer PT. Figure 3.5 shows the simplified equivalent circuit of a PT. The magnitude of the elements in the equivalent circuit are expressed in terms of PT geometry and material characteristics shown in Equation (3.1) –(3.5), and Table 3.1 shows the definitions of the symbols. These equations are essential in the design of a PT for a particular application. Depending on the application requirement, PT can be constructed to have multiple primary and/or secondary layers of different thickness.

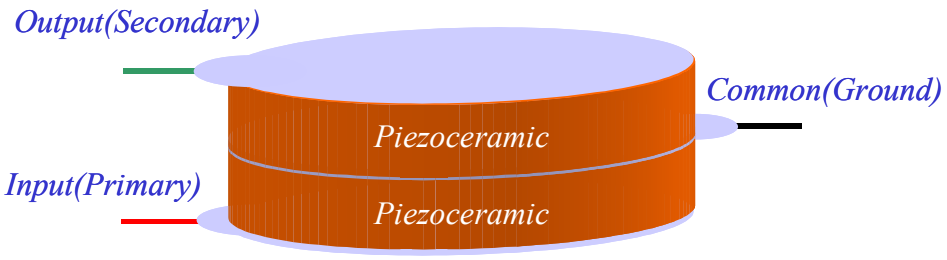

Fig. 3.4. Physical structure of PT.

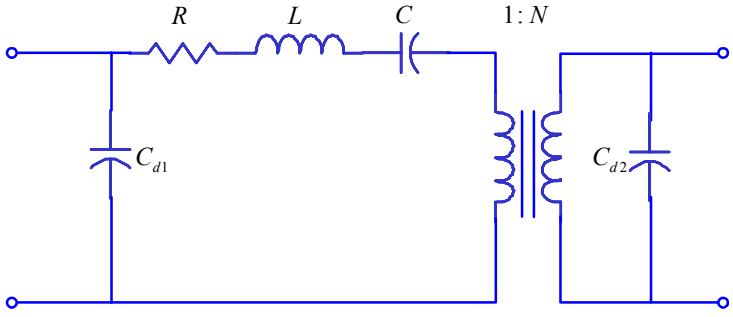

Fig. 3.5. Piezoelectric Transformer equivalent circuit model

The key characteristics of the PT are summarized as follow. The resonant frequency is determined by L, C, and C_{d2} as discussed in chapter 2.

$$C_{d1} = \frac{N_1 \cdot \pi \cdot r^2 \cdot \varepsilon_{33}^T \cdot \left(1 - \frac{{d_{31}}^2}{\varepsilon_{33}^T \cdot S_{11}^E}\right)}{t_1} \tag{3.1}$$

$$R = \frac{\sqrt{2 \cdot \rho \cdot {S_{11}^E}^3} \cdot (N_1 \cdot t_1 + N_2 \cdot t_2)}{16 \cdot r \cdot Q_m \cdot (N_1 \cdot d_{31})^2} \tag{3.2}$$

$$L = \frac{\rho \cdot {S_{11}^E}^2 \cdot (N_1 \cdot t_1 + N_2 \cdot t_2)}{8 \cdot \pi \cdot (N_1 \cdot d_{31})^2} \tag{3.3}$$

$$C = \frac{16 \cdot r^2 \cdot (d_{31} \cdot N_1)^2}{\pi \cdot S_{11}^E \cdot (N_1 \cdot t_1 + N_2 \cdot t_2)} \tag{3.4}$$

$$C_{d2} = \frac{N_2 \cdot \pi \cdot r^2 \cdot \varepsilon_{33}^T \cdot \left(1 - \frac{{d_{31}}^2}{\varepsilon_{33}^T \cdot S_{11}^E}\right)}{t_2} \tag{3.5}$$

$$N = \frac{N_1}{N_2} \tag{3.6}$$

TABLE 3.1 MATERIAL SYMBOLS AND DEFINITIONS

ρ	Density
ε^T_{33}	Permittivity
Q_m	Mechanical Quality Factor
d_{31}	Piezoelectric Coefficient
S^E_{11}	Elastic Compliance
$\tan\delta$	Dissipation Factor
N_R	Radial Mode Frequency Constant
t_1	Primary Layer Thickness
t_2	Secondary Layer Thickness
N_1	Number of Primary Layers
N_2	Number of Secondary Layers
r	Radius of the Layers

It's to be noted that the L, C and C_{d2} in the circuit determine the resonant frequency of the tank circuit. The R value ultimately affects the efficiency of the PT. C_{d1} is not necessary for the circuit but it's inevitable with the PT structure. If a ZVS condition is to be achieved, the charge in C_{d1} has to be discharged when the transistor switch turns on.

3.4 PT Design Requirements and Design Procedure

A. Design Requirement

Table 3.2 summarizes the design specification for the ballast circuit. There are two additional requirements in the design, i.e., zero-voltage-switching of the inverter transistor devices, and unity power factor. The efficiency of the PT is a design input variable, which can be specified by the designers. Matching network can sometimes be added between the PT and the lamp to increase the PT efficiency. However, this will not be considered in this design because it adds additional components to the circuit.

TABLE 3.2 BALLAST CIRCUIT DESIGN SPECIFICATIONS

Circuit Input Voltage (V_{in})	120Vrms 60Hz AC
Rectified DC Bus Voltage (V_{bus})	155V
Lamp Resistance (R_L)	500 Ω
Lamp Power (P_o)	32 W
Voltage gain (A_v)	2.0

From table 3.1, it can be seen that a PT has two kinds of parameters: (1) material parameters: ρ, ε^T_{33}, Q_m, d_{31}, S^E_{11}, tanδ and (2) dimensional parameters: N_1, N_2, t_1, t_2, r. Its equivalent circuit parameter values are highly related to the material and dimensional parameters of the PT.

B. Design Procedure

Step 1. Select the piezoceramic material

Selection of material is mostly based on availability. Once chosen, the materials parameters (ρ, ε^T_{33}, Q_m, d_{31}, S^E_{11}, $\tan\delta$) are given. In this example, APC-841 piezocermic [75] was chosen for the PT with characteristic shown in table 3.3.

TABLE 3.3 PROPERTIES OF APC-841

ρ	7.6 g/cm^3
ε^T_{33}	1350 ε_0
Q_m	1400
$-d_{31}$	109 10^{-12} m/V
S^E_{11}	11.7 10^{-12} m^2/N
N_R	2055 m/s
$\tan\delta$	0.35 %

Step 2. Select the radius r (diameter)

The approximate first radial resonant frequency of the PT can be calculated as equation (3.7) accordingly. [73]:

$$f_r \cong \frac{N_R}{D} = \frac{N_R}{2r} \tag{3.7}$$

Where: N_R, the material waves-speed, is a physical constant. D is the diameter of the PT.

The choice of D is based on several considerations. Since the driving frequency of the inverter is close to the resonant frequency f_r of the PT. Choice of D value essentially fixes the inverter switching frequency. Secondly, choice of D affects the thermal dissipation capability of the PT. Both of them must be considered in choosing D value.

In this design, f_r is chosen to be 98kHz, D is selected as 825-mil.

Step 3. Select number of layers (N_2) of the secondary side.

From (3.6) and the equivalent circuit in Fig 3.2, one can see that the voltage gain of the PT is affected by the ratio of N_1, the number of primary layer and N_2, the number of the secondary layer. This flexibility is available to the designers, just like the turns ratio of a conventional transformer. For the present application, a high voltage gain is needed and therefore, a single layer (N_2=1) will be used.

Step 4. Decide secondary layer thickness t_2

Circuit analysis in chapter 2 reveals that maximum efficiency could be achieved if the load matches the output impedance of PT, i.e., equation (3. 8) is met [50, 72, 76]:

$$R_L = \frac{1}{\omega_s \cdot C_{d2}} \tag{3.8}$$

Each linear fluorescent lamp has a fixed impedance during sustained operation that is considered resistive, as the lamp voltage and current are in phase. By utilizing (3.8) and a given frequency, one can solve for the necessary capacitance, C_{d2}, the PT should exhibit for maximum efficiency.

$$C_{d2} = \frac{1}{\omega_r \cdot R_{LAMP}} = \frac{1}{2\pi \cdot 98 \cdot 10^3 \cdot 500} = 3.2nF \tag{3.9}$$

From equation (3.5), (3.9) and table 3.3.

$$t_2 = \frac{N_2 \cdot \pi \cdot r^2 \cdot \varepsilon_{33}^T \cdot \left(1 - \frac{{d_{31}}^2}{\varepsilon_{33}^T \cdot S_{11}^E}\right)}{C_{d2}} \cong 0.050in = 50mils \tag{3.10}$$

A 60mil was used in the design because of availability.

Step 5. Select number of layers (N_1) of the primary side.

From the previous steps, the output layer is designed. The primary layer number N_1 and thickness t_1 are the two parameters need to be decided in this step. Here t_1 was selected as the design variable, N_1 was iterated until we can meet the following four requirements at the same time: (1) voltage gain requirement, (2) ZVS requirement, (3) efficiency requirement and (4) PFC requirement. That is, N_1 is set to be 1, and check if a proper t_1 can be found to satisfy all four requirements as indicated. If not, then N_1 is set to

2 and repeat. The following paragraph described how a proper t_1 can be found to satisfy the four requirements.

According to the equivalent circuit of PT, the voltage gain of the PT could be calculated as (3.11).

$$A_V = A_V(f_s, t_1) = \left| N \cdot \frac{\left(N^2 / R_{LAMP} + j2\pi f_s N^2 C_{d2}\right)^{-1}}{R + j2\pi f_s L + 1/\left(j2\pi f_s C + \left(N^2 / R_{LAMP} + j2\pi f_s N^2 C_{d2}\right)^{-1}\right)} \right| \qquad (3.11)$$

From (3.1)~(3.6) and (3.11), one can see that once PT material is chosen, and the secondary side parameters N_2, t_2 are fixed then the voltage gain A_v is purely a function of t_1 and f_s. A 3-D plot of A_v vs. the two variables t_1 and f_s (for N_1=1) is shown in Fig. 3.6.

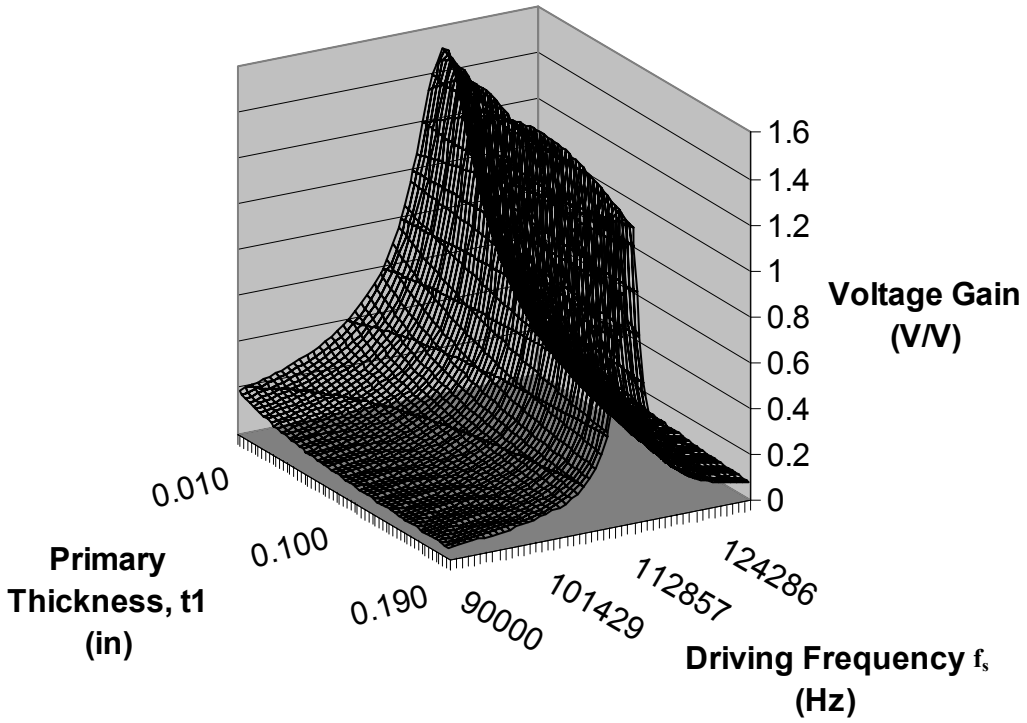

Fig. 3.6. Voltage gain of the PT versus primary layer thickness t_1 and driving frequency f_s, (N_1=1)

By taking a slice of these plots at the minimum voltage gain, two-dimensional surface projections can be generated which allows one to easily see where in the (t_1 x f_s) plane a solution exists as shown in Fig. 3.7, where the red area meets the requirement.

Similarly, three other two-dimensional surface projections can be generated to check whether the efficiency requirement, the ZVS requirement and the PFC requirement are met. In order to create the smallest range of choices for primary layer thickness, the four plots are then overlapped to find the common choices of both t_1 and f_s, which are elements of all four two-dimensional projections. Any choice within this overlapped region will provide a useful PT that satisfies all the four requirements. In the design process, if no solution can be found, then increase N_1 by one and check again until a solution is found. The details of the four requirements are described as follow.

A. Voltage gain requirement

According to the design specification, the required voltage gain is approximately 2.0 V/V. Figure 3.6 shows that no solution can be found because $A_v<2$ for the whole range. So N_1 needs to be increased to meet the voltage gain requirement. Fig 3.7 shows the region where the voltage gain requirement was met when the N_1 was increased to 4.

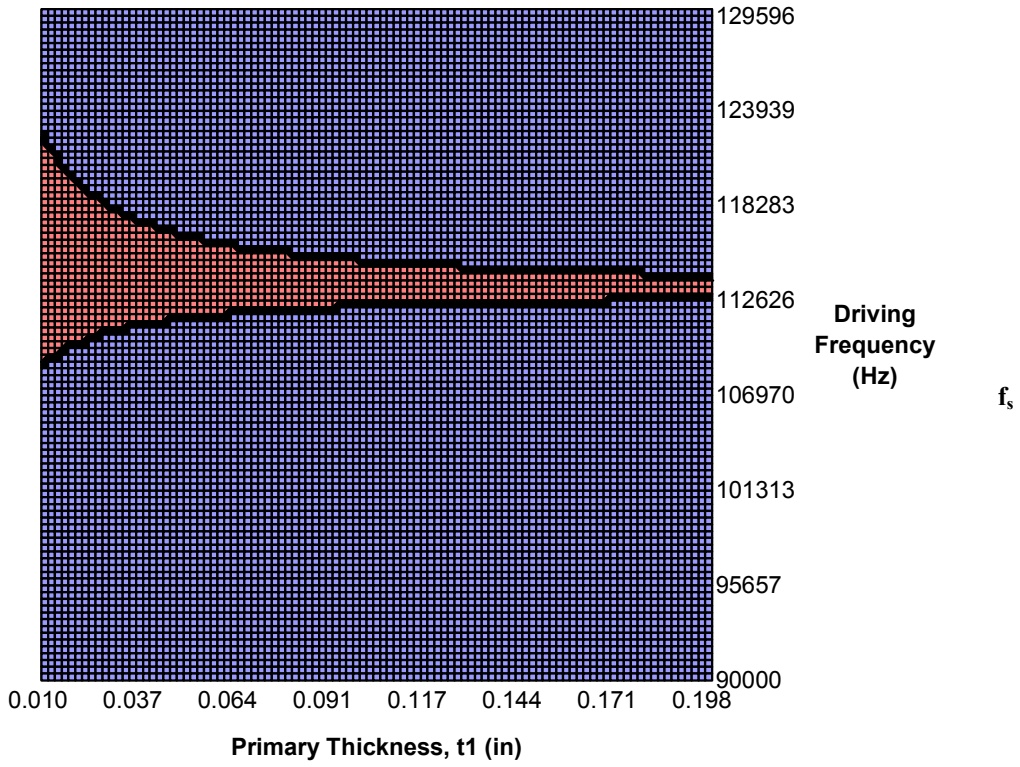

Fig. 3.7. Region where voltage gain is greater than the minimum requirement (N_1=4)

B. ZVS requirement

In order to achieve Zero Voltage Switching (ZVS), enough energy is needed to charge/ discharge the input capacitor, C_{d1}, sufficient dead time is also needed for the resonance, as shown in equation (3.12-3.13) [4, 73]. Fig. 3.8 shows the region in which ZVS requirement can be meet.

$$\Delta i_{L\,peak}(t_1, f_s) \geq \sqrt{\frac{C_{d1}(t_1)\cdot(C(t_1)+C_{d1}(t_1)}{L(t_1)\cdot C(t_1)}}\cdot V_{bus} \tag{3.12}$$

where

$$\Delta i_{L\,peak}(t_1, f_s) = \frac{2\cdot V_{bus}}{\pi\cdot\left|Z_{in}(t_1, f_s)\right|}\cdot\frac{\sin(\pi\cdot d)}{\pi\cdot d}\sin(\angle Z_{in}(t_1, f_s)) \tag{3.13}$$

In (3.13), Z_{in} is input impedance excluding the input capacitor C_{d1}, and f_s is the switching frequency of the half-bridge.

Using V_{bus}=155V and Equation (3.1)~(3.6), the left-hand side of (3.12), $\Delta i_{L\,peak}(t_1, f_s)$, can be expressed in terms of t_1 and f_s. The parameters C_{d1}, C, and L on the right-hand side of (3.12) can also be found by using (3.1)~(3.6). The region that satisfies (3.13) is shown by the red area in Fig. 3.8.

C. Efficiency requirement

One other consideration should be for efficiency. Efficiency of the PT can be represented by (3.14), η_{spec} is a user specified number. In this example, η_{spec} is chosen to 90%, and N is an integer. As indicated earlier, N_1 is iterated from one upward until a common solution that satisfies voltage gain requirement, ZVS condition and efficiency requirement. In this example, N_1=4. The efficiency plot is given in Fig. 3.9.

$$\eta(f_s, t_1) = \frac{1}{1+\left[1+(2\pi f_s R_L)^2\right]\cdot\frac{N^2 R(t_1)}{R_L}} \geq \eta_{spec} \tag{3.14}$$

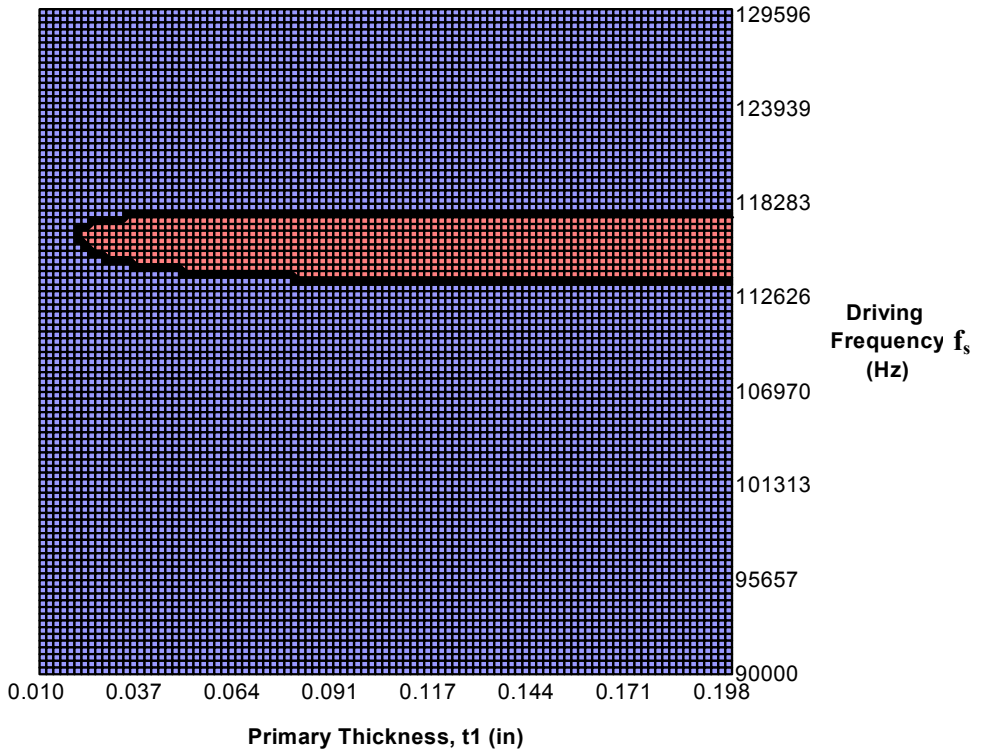

Fig. 3.8. Region where ZVS requirement can be met (N_1=4).

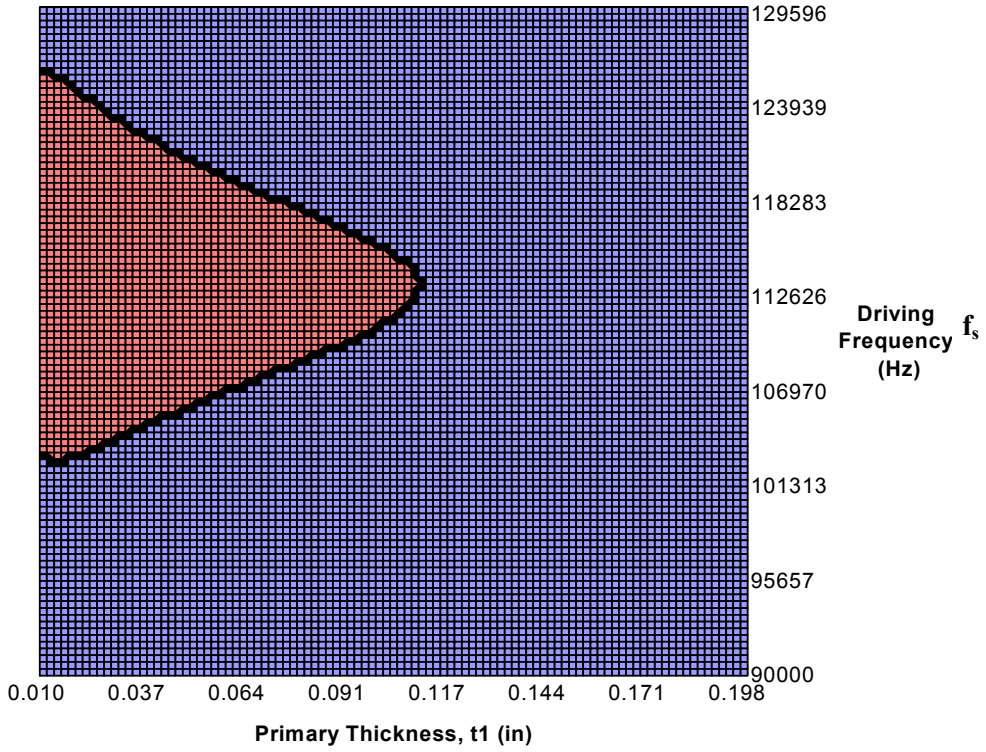

Fig. 3.9. Region where efficiency is greater than the preset minimum. (N_1=4)

D. PFC requirement

In the PT design process for charge pump PFC ballast application, another constraint, PFC constraint, was incorporated to further narrow the t_1 range.

According to [4], the condition for unite power factor for this charge pump PFC ballast circuit is shown in (3.15)

$$I_s \geq \pi \cdot \left(C_{in} + 2C_{d1}\right) \cdot f_s \cdot V_{bus} \tag{3.15}$$

where I_s is the resonant current, C_{in} can be calculated using (3.16) [4]. To use this information for a PT design, (3.17) is obtained by substituting (3.15) by into (3.16).

$$C_{in} = \frac{2P_o}{\eta f_s V_{in-peak}^2} - C_{d1} \tag{3.16}$$

$$I_s(f_s, t_1) \geq \pi \cdot \left(\frac{2P_o}{\eta f_s V_{in-peak}^{\ 2}} + C_{d1}(t_1) \right) \cdot f_s \cdot V_{bus} \tag{3.17}$$

Similarly, the region where PFC requirement is met can be plotted, as shown in Fig. 3.10.

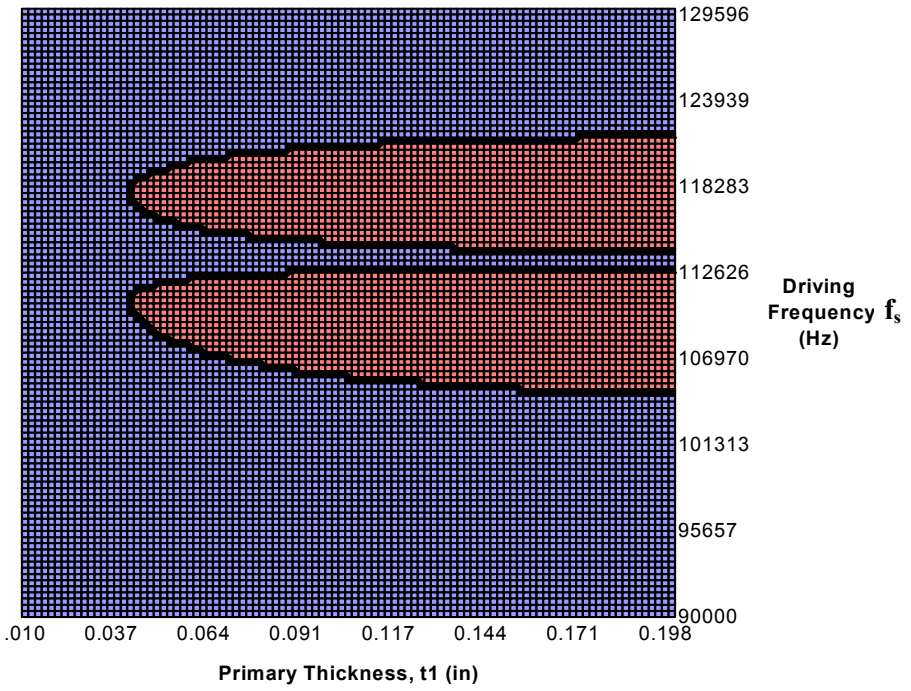

Fig. 3.10. Region where PFC requirement can be meet (N_1=4)

E. Solution

By overlapping the red regions in Fig. 3.7 –Fig. 3.10, a solution region can be found. In other words, this region satisfies all the design requirements. In this design, when the primary layers were increased to four, solution can be found. The completed solution region in the (t_1 x f_s) space was shown in Fig. 3.11. Selecting a point within the solution region gives a workable design.

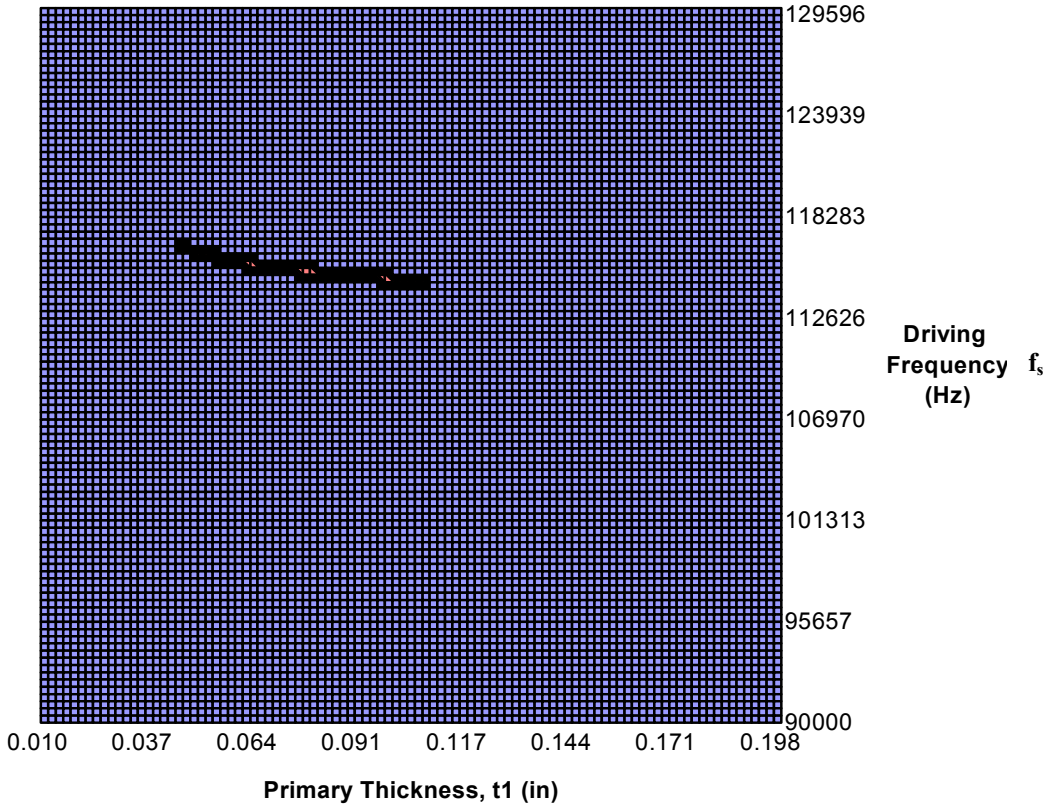

Fig. 3.11. Valid Choices for the prototype PT.

Step 6. Design of the primary layer thickness t_1

From Fig. 3.11, solution point of t_1=60mils and f_s=116 kHz is chosen for design. A comparison of different design is possible but is not done in this approach because the sample material available to us was 60mils.

Step 7. Construct the whole PT

By adding input, output and ground terminal wire, the entire PT was constructed. The complete PT has four primary layers of 60-mil each and a secondary layer of 60-mil. The overall diameter is 825-mil. A simple diagram of the prototype is shown as Fig. 3.12 with the theoretical equivalent circuit model parameters shown within Table 3.4. The new designed PT looks much more attractive than CZ-3, as shown in Fig. 3.13.

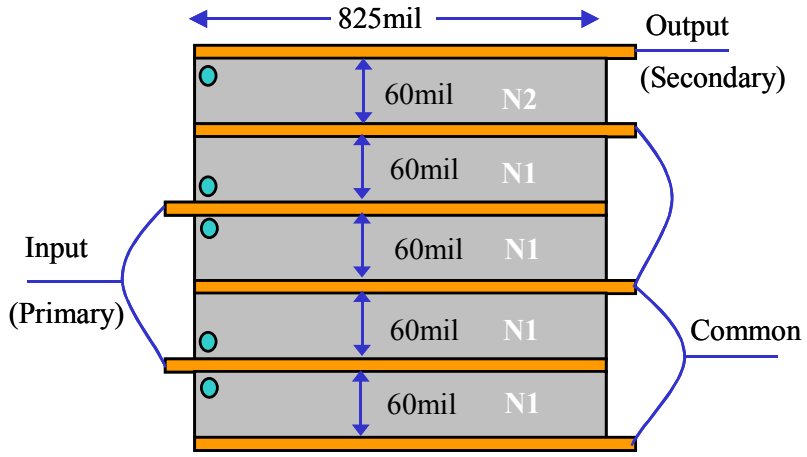

Fig. 3.12. Physical construction of the prototype PT (VTE-1).

TABLE 3.4 THEORETICAL EQUIVALENT CIRCUIT PARAMETERS OF VTE-1

C_{d1}	R	L	C	C_{d2}	N
9.9nF	0.843 Ω	1.659 mH	1.192 nF	2.475 nF	4

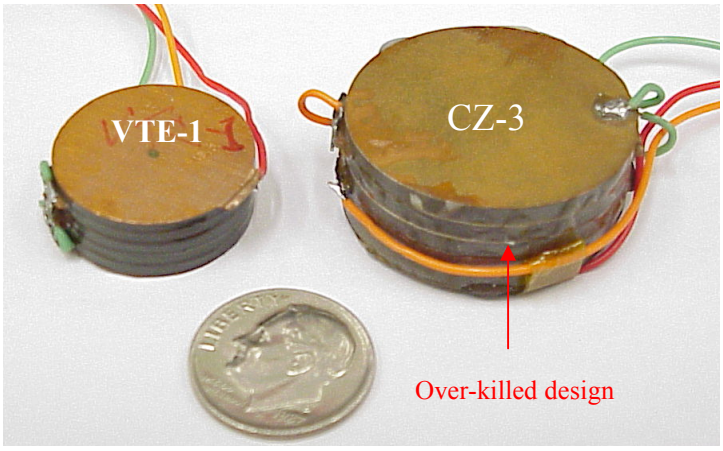

Fig. 3.13. CZ-3 Vs. VTE-1

For better understanding of the design process, a flow chart was shown in Fig 3.14 to summarize the whole design process.

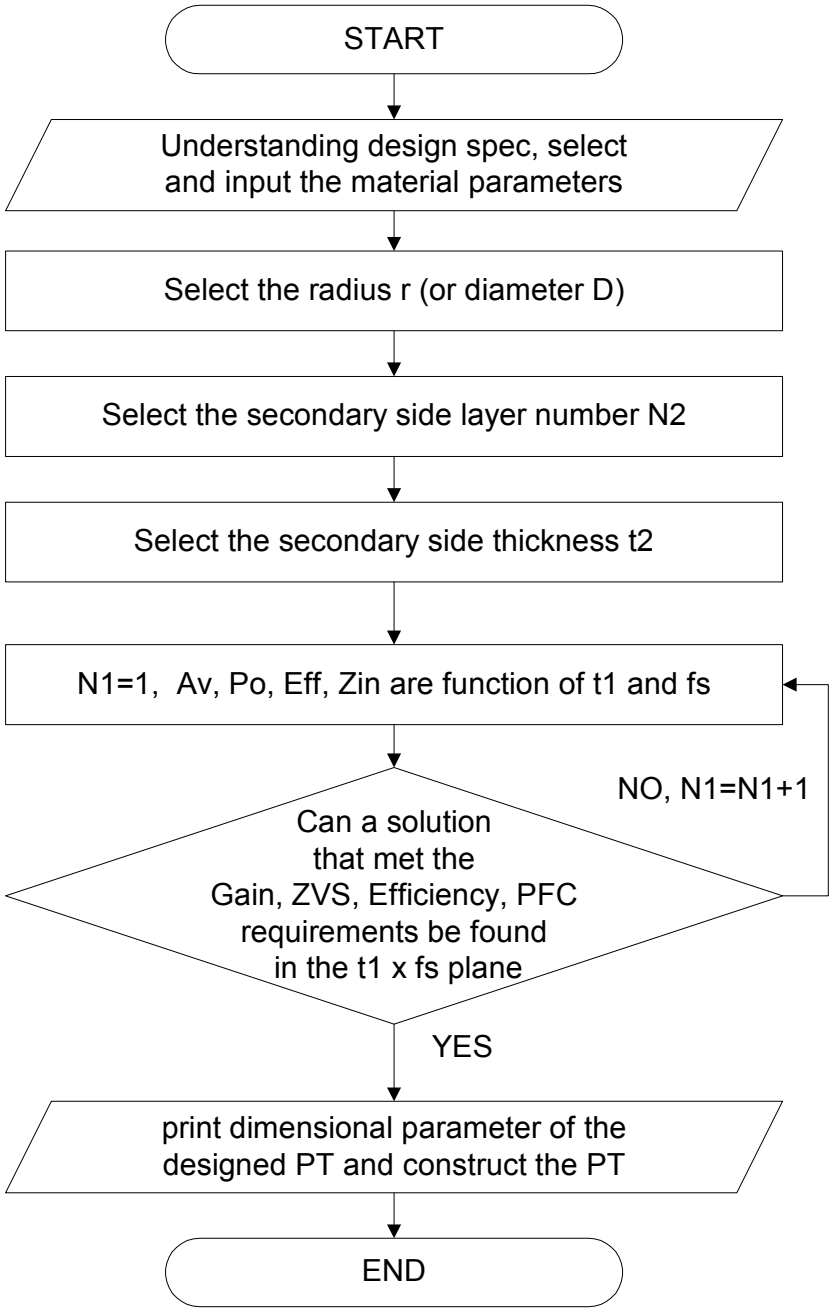

Fig. 3.14. Flow-chart of designing the piezoelectric transformer for PFC ballast

Simulation result shows that both ZVS and PFC can be achieved by using the theoretical parameters of the designed PT, as shown in Fig 3.15. In the simulation, a load

resistor of 500 Ω was used to simulate the steady-state lamp reistance. This can also be verified by the experimental results provided in the following section.

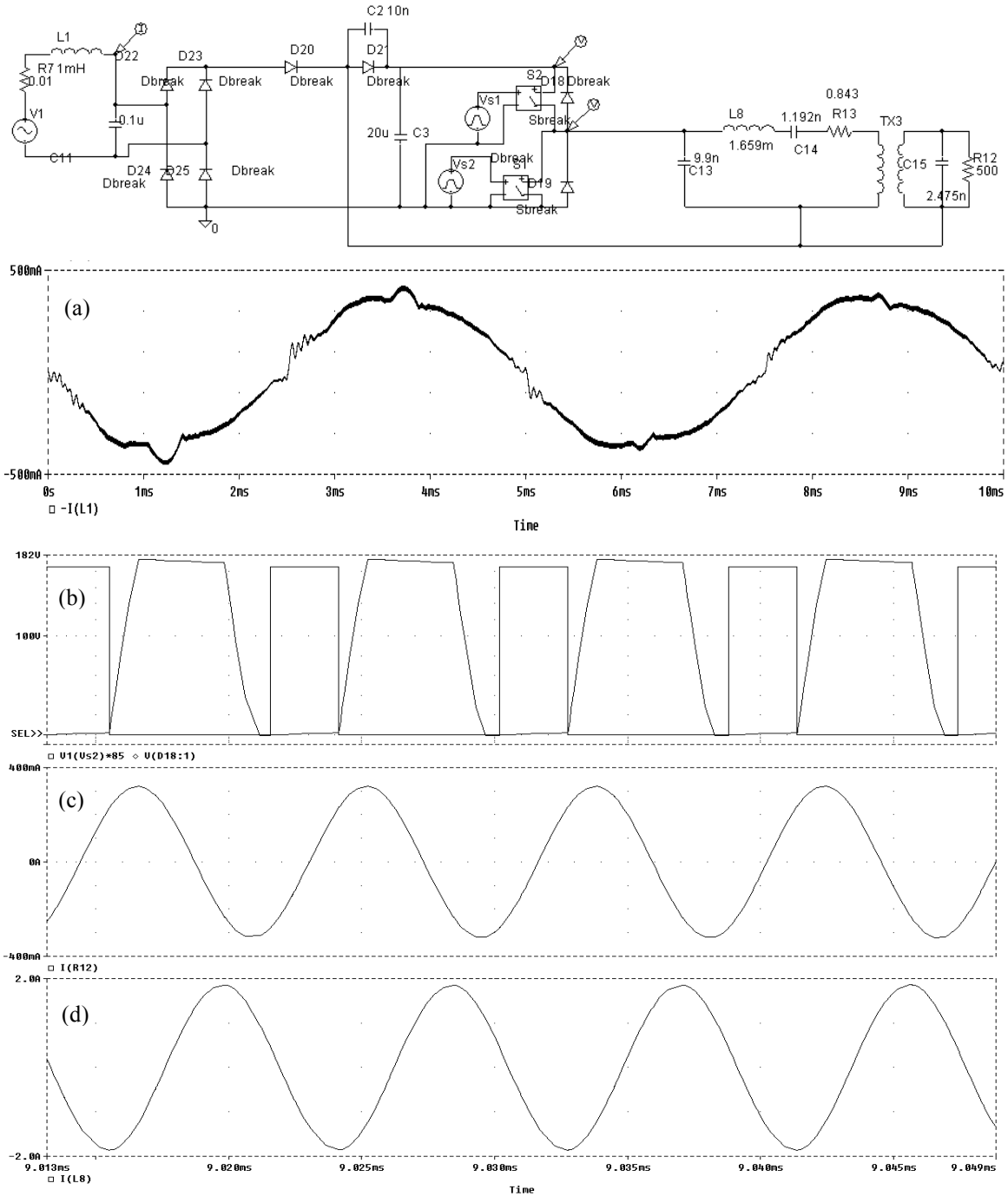

Fig. 3.15. Simulation results. (a)Input line current (b) Switch voltage V_{DS} (c) Output current (d) Resonant inductor current

3.5 Experimental Results

A. Parameter measurement results of the designed PT

In order to verify the design procedure, a sample design was fabricated by Face Electronics Inc. The measured equivalent circuit parameters appear in Table 3.5. As can be seen, the parameters match well except for the equivalent internal inductance and capacitance. But the resonant frequency does not vary much.

TABLE 3.5 MEASURED VTE-1 EQUIVALENT CIRCUIT PARAMETERS

C_{d1}	R	L	C	C_{d2}	N
8.8 nF	1.068 Ω	1.004 mH	2.403 nF	2.308 nF	4.79

Further analysis reveals that the performance of the theoretical model and the measured model is close. Figs. 3.16-3.18 show both the theoretical and actual performance, based on the equivalent circuit models, predicting voltage gain during steady state operation, efficiency, and inductor current, respectively, when a load of 500-ohms is attached to the outputs. The discrepancy in resonant frequency is less than 10%.

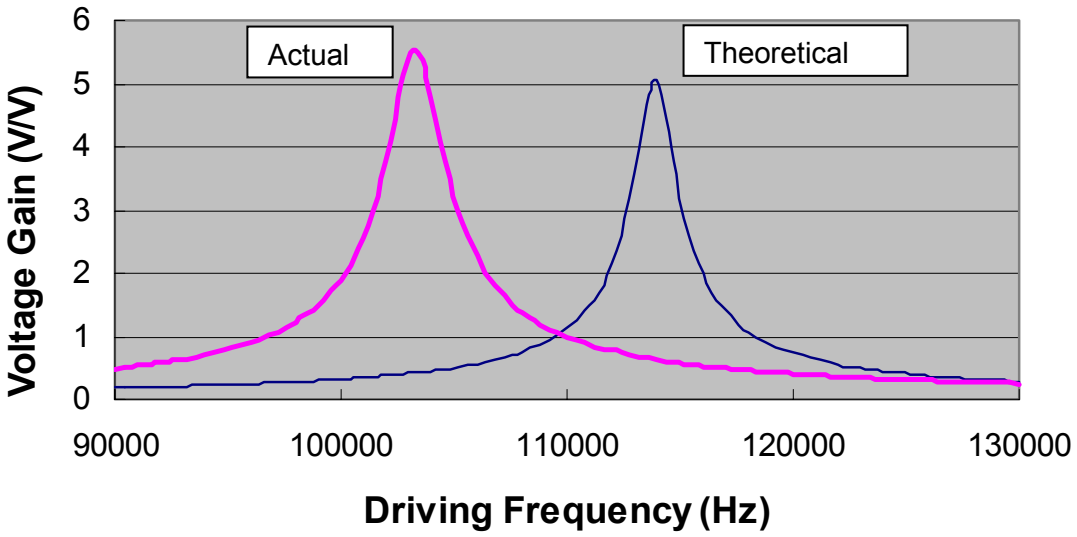

Fig. 3.16. Comparison of theoretical and actual steady-state voltage gain for VTE-1

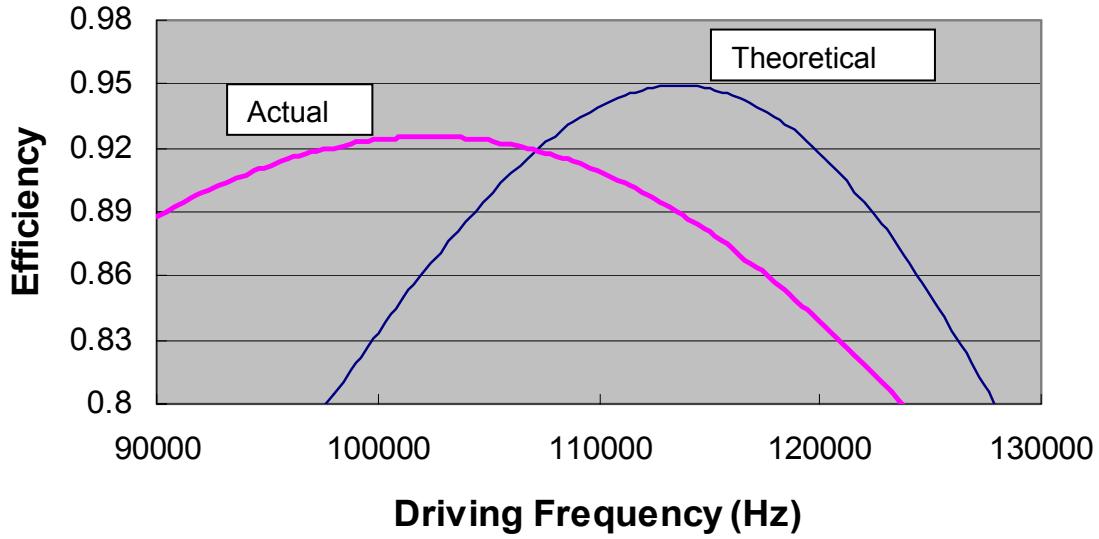

Fig. 3.17. Comparison of theoretical and actual efficiency

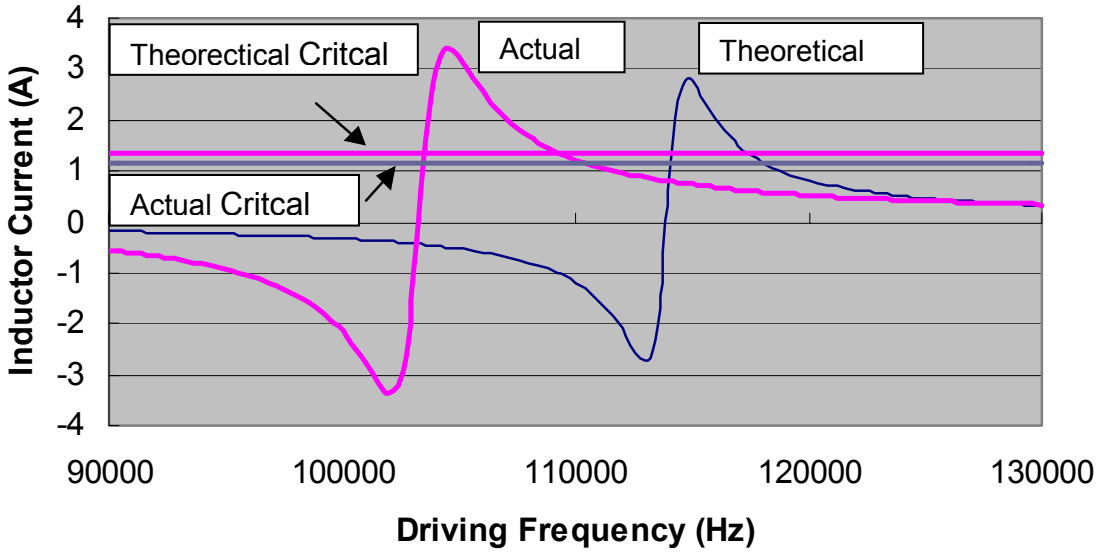

Fig. 3.18. Comparison of theoretical and actual inductor current.

From Fig. 3.17, One can find that the actual efficiency of VTE-1 is lower than that of the theoretical efficiency, this is due to the discrepancy of internal resistance values.

B. *Ballast circuit experimental results*

An inductor-less Current Source Charge Pump Power Factor Correction (CSCPPFC) electronic ballast was constructed using this custom-designed PT. Fig. 3.19 shows the picture of the PFC ballast. Notice the disk with clamp on the right corner of the circuit board is the custom made PT designed based on the proposed procedure in this thesis. Fig. 3.20 shows the 60-Hz AC input voltage to the circuit and the respective input current. As can been seen from the waveforms, both the line voltage and line current are in phase and relatively sinusoidal, the circuit with the custom designed PT operates close to unite power factor. Measurement of the power factor yields an operation point of 0.987 with an input current harmonic distortion equal to 9.7%, and each harmonic component satisfies IEC1000-3-2 class C requirements as shown in Fig. 3.21. By viewing the voltage across the bottom switch, as shown in Fig. 3.22, one can determine that the switches are operating in a zero voltage switching condition. The duty cycle for each switch is set to approximately 25%. During the dead-time period, the current in the inductor charges/discharges the piezoelectric transformer input capacitor, C_{d1} and the MOSFET drain-source capacitances. Here we can see that the voltage transitions in a sinusoidal manner from the bus to ground during one portion of the dead-time period and from ground back to the bus during the other period. At the time when the transition tries to exceed the bus voltage or go below the ground reference, the body diode of the respective MOSFET conducts. During the body diode conduction, the voltage across the switch is virtually zero. If the switch is turned on during this condition the turn-on switching losses are minimized Efficiency measurement shows that the circuit can achieve efficiency as high as 83%.

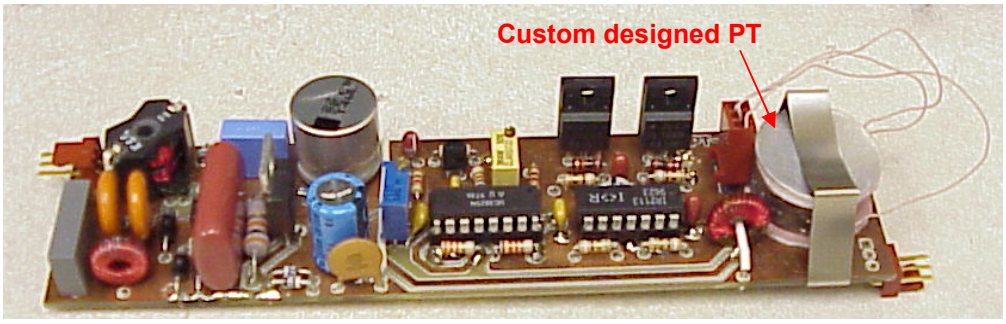

Fig. 3.19. The prototype of the proposed PFC ballast

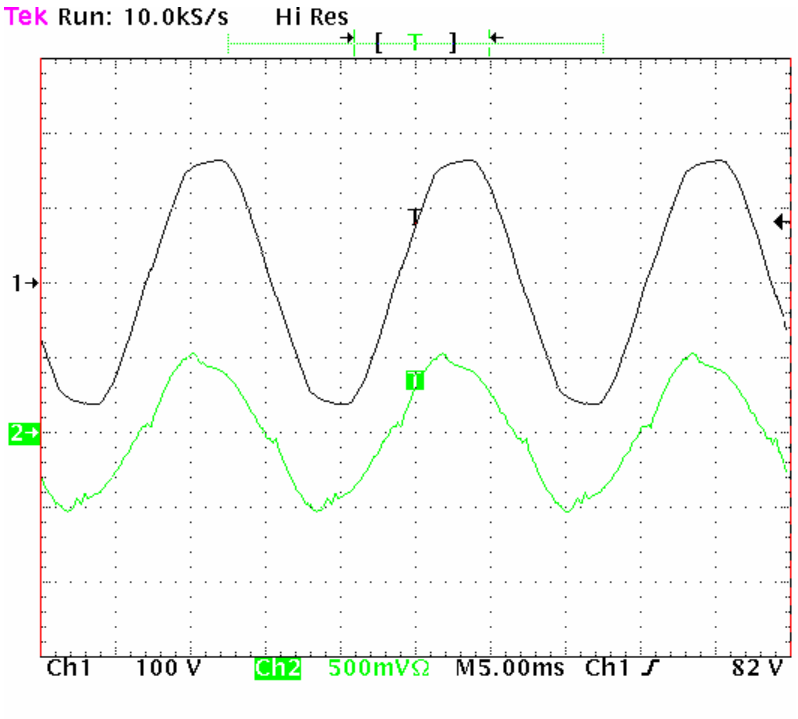

Fig. 3.20. Line voltage and line current to the PFC circuit.

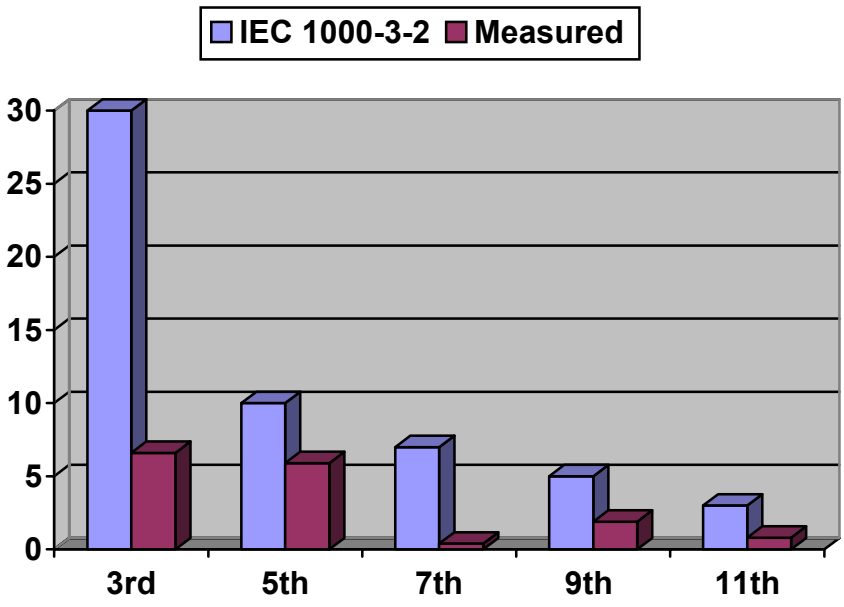

Fig. 3.21. Input current harmonics compared with IEC1000-3-2 Class C requirements

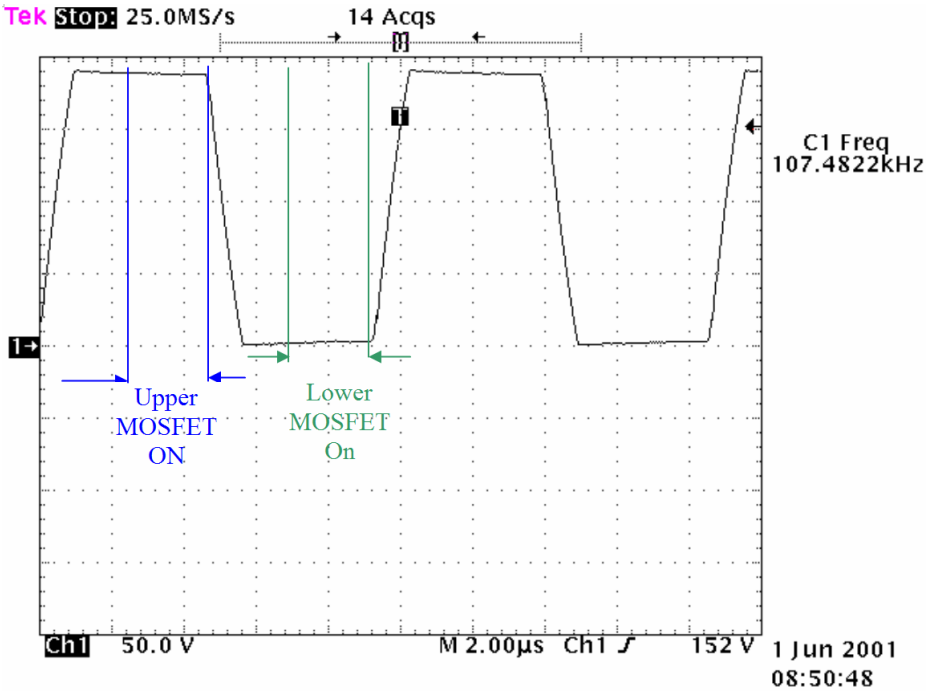

Fig. 3.22. Bottom switch drain-to-source voltage displaying ZVS operation.

3.6 Conclusions

A procedure has been proposed for designing a Piezoelectric Transformer (PT) tailored for a 32W inductor-less electronic ballast circuit. The circuit achieves zero-voltage-switching and high efficiency as well as high power factor. The complicated relationships among PT parameters and ballast circuit performance make it compelling to design the PT with reasonably accurate mathematical model to achieve desirable performance. An over-killed design often is larger in size but also leads to larger circulating current in the PT therefore greatly degrade the efficiency. The paper proposes a design procedure to achieve high performance.

CHAPTER 4 CONCLUSIONS AND FUTURE WORKS

Several conclusions were drawn from this investigation:

1. The proposed design procedure proves to be very effective in designing a piezoelectric transformer for a given ballast circuit requirements. Because of the numbers of parameters involved and the intertwine relationships, it is very difficult for a designer to come up with a PT design that can meet all the requirement. The proposed procedure provides an efficient and practical way of accomplishing such.

2. A PT prototype based on the proposed design procedure work very well with the ballast circuit. Power factor of near unity, efficiency of 83% and zero-voltage-switching are all achieved. It is also observed that the actual measurement results agree well the simulation results. This confirms the validity of the PT model.

3. It is observed that radial mode PT characteristics match lamp resistance so that high efficiency can be achieved. Other types of PT do not match as well.

Suggestion for future research:

1. Matching network to improve efficiency is not considered in this application because it is not necessary. The output characteristic of these PTs match well with lamp characteristics. However, for other applications where the load resistance does not match well, matching network maybe necessary to obtain reasonable overall efficiency. Further research should be done alone this line.

2. It is suggested future research to be conducted to extend the concept proposed in this thesis to DC/DC converter applications. PT is basically sharply-tuned LC resonant circuit which is also used often in many resonant DC/DC conversion applications.

REFERENCES

[1] Jiyuan Luan, "Design Development of High Frequency Switching Amplifiers Used for Smart Material Actuators With Current Mode Control", M.S. Thesis, Virginia Tech, July, 1998

[2] C. A. Rosen, “Analysis and Design of Ceramic Transformer Transformers and Filter Elements,” Ph.D. Dissertation, Electrical Engineering Dept., Syracuse University, August 1956.

[3] C. A. Rosen, “Ceramic Transformers and Filters,” Proc. of Electronic Comp. Symp., pp. 205-211, 1956.

[4] Jinghai Zhou, Fengfeng Tao, Fred C. Lee, “Inductor-less Charge Pump PFC Electronic Ballast”, 2001 IEEE Industry Application Conference, pp. 524~529.

[5] Ray-Lee Lin, Fred C. Lee, Eric M. Baker, Dan Y. Chen, “Inductor-less piezoelectric transformer electronic ballast for linear fluorescent lamp”, IEEE APEC 2001, pp. 664~669.

[6] Moo, C.S.; Chen, W.M.; Hsieh, H.K.; “An electronic ballast with piezoelectric transformer for cold cathode fluorescent lamps”, Proceedings of ISIE 2001, Volume: 1, pp. 36~41, 2001

[7] Lee, J.S.; Lee, Y.H.; Chai, H.I.; Yoon, M.S.; Lim, K.J.; “The characteristics of new piezoelectric ballast for fluorescent T8 lamp”, Proceedings of ISIE 2001, Volume: 2, pp. 947~951, 2001.

[8] Gie Hyoun Kweon; Young Cheol Lim; Seung Hak Yang; “An analysis of the backlight inverter by topologies”, Proceedings of ISIE 2001, Volume: 2, pp. 896~900, 2001

[9] Yoo, J.-H.; Hwang, S.-M.; Min, S.-K.; Yoon, K.-H.; Suh, S.-J.; Kim, J.-S.; “High power piezoelectric transformer for driving a 28 W fluorescent lamp”, Proceedings of the 2000 12th IEEE International Symposium on Applications of Ferroelectrics, ISAF 2000, Volume: 2, pp. 709~712, 2001

[10] Jin-Hong Chung; Seung-Min Lee; Mike Myung-Ok Lee; Yang Ho Moon; “High power 30 W and high efficiency 80% piezoelectric transformer for EB”, The First IEEE Asia Pacific Conference on ASICs, 1999. AP-ASIC '99, pp. 131~134, 1999

[11] Kakehashi, H.; Hidaka, T.; Ninomiya, T.; Shoyama, M.; Ogasawara, H.; Ohta, Y.; “Electronic ballast using piezoelectric transformers for fluorescent lamps”, PESC 98, pp. 295~299, 1998

[12] Sung-Jin Choi; Kyu-Chan Lee; Cho, B.; “Design of fluorescent lamp ballast with PFC using a power piezoelectric transformer”, APEC '98, Volume: 2, pp. 1135~1139, 1998

[13] Shoyama, M.; Horikoshi, K.; Ninomiya, T.; Zaitsu, T.; Sasaki, Y.; “Steady-state characteristics of the push-pull piezoelectric inverter”, PESC '97, Volume: 1, pp. 715~721 1997.

[14] Shoyama, M.; Horikoshi, K.; Ninomiya, T.; Zaitsu, T.; Sasaki, Y.; “Operation analysis of the push-pull piezoelectric inverter”, APEC'97, Volume: 2 , pp.573~578, 1997

[15] Doo-Oh Hur; Tae-Ku Kang; Cheol-Hwan Cho; Hae-Min Lee; Hyung-Keun Ahn; Deuk-Young Han; “Design and fabrication of piezoelectric ceramic transformers for the LCD backlight”, Proceedings of the 5th International Conference on Properties and Applications of Dielectric Materials, 1997, Volume: 2, pp. 843~846, 1997

[16] Zaitsu, T.; Fuda, Y.; Okabe, Y.; Ninomiya, T.; Hamamura, S.; Katsuno, M.; "New piezoelectric transformer converter for AC-adapter", APEC'97, Volume: 2, pp. 568~572, 1997

[17] Navas, J.; Bove, T.; Cobos, J.A.; Nuno, F.; Brebol, K.; "Miniaturised battery charger using piezoelectric transformers", APEC 2001, Volume: 1, pp. 492~496, 2001.

[18] Vasic, D.; Costa, F.; Sarraute, E.; "A new MOSFET & IGBT gate drive insulated by a piezoelectric transformer", IEEE PESC. 2001, Volume: 3, pp. 1479~1484, 2001

[19] Sam Ben-Yaakov, Moshe Shvartsas and Gregory Ivensky, "A Piezoelectric Cold Cathode Fluorescent Lamp Driver Operating from a 5 Volt Bus", PCIM 2000, pp. 379~383.

[20] Dallago, E.; Danioni, A.; Passoni, M.; Venchi, G.; "Modelling of DC-DC converter based on a piezoelectric transformer and its control loop", IEEE PESC 02, Volume: 2, pp. 927~931.

[21] Dallago, E.; Danioni, A.; "Resonance frequency tracking control for piezoelectric transformer DC-DC converter", Electronics Letters , Volume: 37 Issue: 22 , pp. 1317~1318, 25 Oct. 2001.

[22] Prieto, M.J.; Diaz, J.; Martin, J.A.; Nuno, F.; "A very simple DC/DC converter using piezoelectric transformer", IEEE PESC. 2001, Volume: 4, pp. 1755~1760, 2001

[23] Martin, J.A.; Prieto, M.J.; Nuno, F.; Diaz, J.; "A new full-protected control mode to drive piezoelectric transformers in DC-DC converters", IEEE PESC. 2001, pp. 378~383, 2001

[24] Hamamura, S.; Zaitsu, T.; Ninomiya, T.; Shoyama, M.; "Noise characteristics of piezoelectric-transformer DC-DC converter", PESC 98, Volume: 2, pp. 1262~1267, 1998

[25] Yamane, T.; Hamamura, S.; Zaitsu, T.; Minomiya, T.; Shoyama, M.; Fuda, Y.; "Efficiency improvement of piezoelectric-transformer DC-DC converter", PESC 98, pp. 1255~1261, 1998

[26] Imori, M.; Taniguchi, T.; Matsumoto, H.; "Performance of a photomultiplier high voltage power supply incorporating a piezoelectric ceramic transformer", IEEE Transactions on Nuclear Science; Volume: 47 Issue: 6 Part: 2, pp. 2045~2049, Dec. 2000

[27] Imori, M.; Taniguchi, T.; Matsumoto, H.; "A photomultiplier High-Voltage power supply incorporating a piezoelectric ceramic transformer Driven by Frequency Modulation", IEEE Transaction on Nuclear Science, Volume 45, No. 3, pp. 777~781, June 1998

[28] Imori, M.; Taniguchi, T.; Matsumoto, H.; Sakai, T.; "A photomultiplier high voltage power supply incorporating a piezoelectric ceramic transformer", IEEE Transactions on Nuclear Science, Volume: 43 Issue: 3 Part: 2, pp. 1427~1431, June 1996

[29] Thomas Hanisch, Igor Kartashev and Henry Gueldner, "Piezoelectric Transformer operation in Ignition System", The 6th Brazilian Power Electronics Conference, COBEP'2001, pp. 255~258

[30] Mutoh, A.; Nitta, S.; Mitani, T.; "A feasibility study on the application of piezoelectric transformer to pulse shaping circuit", International Symposium on Electromagnetic Compatibility, 2001. EMC 2001, Volume: 2, pp. 1072~1077, 2001

[31] Hyeoung woo Kim, Shuxiang Dong, et al, "Novel method for driving the ultrasonic motor", IEEE Transactions on Ultrasonics, Ferroelectrics and Frequency Control, Vol. 49 Issue: 10, pp. 1356~1362.

[32] Alfredo V. Azquez Carazo and Kenji Uchnino, “Novel Piezoelectric-Based Power Supply for Driving Piezoelectric Actuators Designed for Active Vibration Damping Applications”, Journal of Electroceramics, 7, 197–210, 2001

[33] K. Uchino, B. Koc, et al, “Piezoelectric Transformers--New Perspective”, Ferroelectrics, 2001, Vol. 263, pp 91~100.

[34] Itoh, H.; Teranishi, K.; Suzuki, S.; “Observation of light emissions around a piezoelectric transformer in various gases”, IEEE Transactions on Plasma Science, Vol. 30 Issue: 1, pp. 124~125.

[35] Teranishi, K.; Itoh, H.; Suzuki, S.; “Dynamic behavior of light emissions generated by piezoelectric transformers”, IEEE Transactions on Plasma Science, Vol: 30 Issue: 1, pp. 122~123.

[36] B. Jaffe, “Piezoelectric Ceramics”, New York, Academic Press, 1971, pp. 1-5.

[37] Michel Brissaud, “Characterization of Piezoceramics”, IEEE Transactions on Ultrasonics, Ferroelectrics and Frequency Control, Vol. 38, No. 6, Nov. 1991, pp. 603~617

[38] Ray-Lee Lin, “Piezoelectric Transformer Characterization and Application of Electronic Ballast,” Ph.D. Dissertation, Virginia Tech, November 2001.

[39] Syed, E.M.; Dawson, F.P.; Rogers, E.S., Sr.; “Analysis and modeling of a Rosen type piezoelectric transformer”, IEEE PESC. 2001, Volume: 4, pp. 1761~1766, 2001

[40] Fukunaga, H.; Kakehashi, H.; Ogasawara, H.; Ohta, Y.; “Effect of dimension on characteristics of Rosen-type piezoelectric transformer”, PESC 98, Volume: 2, pp. 1504~1510, 1998

[41] C. A. Rosen, US Patent 2,974,296, March 1961.

[42] Zaitsu, T.; Ohnishi, O.; Inoue, T.; Shoyama, M.; Ninomiya, T.; Lee, F.C.; Hua, G.C., “Piezoelectric transformer operating in thickness extensional vibration and its application to switching converter”, PESC '94, pp. 585~589, 1994

[43] Ohnishi, O.; Kishie, H.; Iwamoto, A.; Sasaki, Y.; Zaitsu, T.; Inoue, T.; “Piezoelectric ceramic transformer operating in thickness extensional vibration mode for power supply”, Proceedings, IEEE 1992 Ultrasonics Symposium, Vol. 1, pp. 483~488, 1992.

[44] Zaitsu, T.; Inoue, T.; Ohnishi, O.; Iwamoto, A.; “2 MHz power converter with piezoelectric ceramic transformer”, 14th International Telecommunications Energy Conference, INTELEC '92, pp. 430~437, 1992

[45] T. Inoue, S. Ohnishi, N. Ohde, “Thickness Mode Vibration Piezoelectric Transformer.” U.S Patent 8,118,982, Jun 2, 1992.

[46] Eric M. Baker, “Design of Radial Mode Piezoelectric Transformers for Lamp Ballast Applications”, M.S. Thesis, Virginia Tech, May, 2002

[47] Ray L. Lin, Eric Baker, and Fred C. Lee, “Transoner Characterization”, First Quarterly Progress Report, ELC-99-007, August 28, 1999.

[48] Ray L. Lin, Eric Baker, Jia Wei, Dan Y. Chen, and Fred C. Lee, “Transoner Characterization”, Second Quarterly Progress Report, ELC-99-007, Oct. 29, 1999.

[49] Ray L. Lin, Eric Baker, Jia Wei, Dan Y. Chen, and Fred C. Lee, “Transoner Characterization”, Third Quarterly Progress Report, ELC-99-007, Jan. 31, 2000.

[50] Ray L. Lin, Eric Baker, Jia Wei, Dan Y. Chen, and Fred C. Lee, “Transoner Characterization”, Final Report, ELC-99-007, April. 31, 2000.

[51] Eric M. Baker, Fengfeng Tao, Weixing Huang, Jinghai Zhou, Dan Y. Chen and Fred C. Lee, “Linear Ballast Development”, First Quarterly Report, ELC-00-006, September 30, 2000

[52] Eric M. Baker, Jinghai Zhou, Fengfeng Tao, Weixing Huang, Dan Y. Chen and Fred C. Lee, “Linear Ballast Development”, Second Quarterly Report, ELC-00-006, December 30, 2000

[53] Eric M. Baker, Jinghai Zhou, Weixing Huang, Fengfeng Tao, Dan Y. Chen and Fred C. Lee, “Linear Ballast Development”, Third Quarterly Report, ELC-00-006, February 28, 2001

[54] Eric M. Baker, Jinghai Zhou, Weixing Huang, Fengfeng Tao, Dan Y. Chen and Fred C. Lee, “Linear Ballast Development”, Final Report, ELC-00-006, May 31, 2001

[55] Eric M. Baker, Weixing Huang, Dan Y. Chen and Fred C. Lee, “Piezoelectric Transformer based Circuit Techniques for Power Applications”, Final Report for Panasonic, Aug 9, 2001

[56] Bove, T.; Wolny, W.; Ringgaard, E.; Breboel, K.; “New type of piezoelectric transformer with very high power density”, Proceedings of ISAF 2000, Volume: 1, pp. 321~324, 2001

[57] Koc, B.; Alkoy, S.; Uchino, K.; “A circular piezoelectric transformer with crescent shape input electrodes”, Proceedings. 1999 IEEE Ultrasonics Symposium, 1999, Volume: 2, pp. 931~934, 1999

[58] Sakurai, K.; Shindou, S.; Ohnishi, K.; Tomikawa, Y.; “Piezoelectric ceramic transformer using radial vibration mode disks”, Proceedings., 1998 IEEE Ultrasonics Symposium, 1998, Volume: 1, pp. 939~944, 1998

[59] Pitak Laoratanakul, Alfredo Vazquez Carazo,et al, “Unipoled Disk-type Piezoelectric Transformers”, Japanese Journal of Applied Physics, Vol. 41, Part 1., No. 3A, March 2002, pp. 1446~1450.

[60] Yoo, J.-H.; Lee, Y.-W.; Hwang, S.-M.; Yoon, H.-S.; Jeong, H.-S.; Kim, J.-S.; Yoo, C.-S.; “Piezoelectric properties of PNW-PMN-PZT ceramics for high power piezoelectric transformer”, Proceedings of ISAF 2000, Volume: 1, pp. 495~498, 2001

[61] Prieto, R.; Sanz, M.; Cobos, J.A.; Alou, P.; Garcia, O.; Uceda, J.; “Design considerations of multi-layer piezoelectric transformers”, APEC 2001, Volume: 2, pp. 1258~1263, 2001

[62] Hu, J.H.; Li, G.R.; Chan, H.L.W.; Choy, C.L.; “An improved method for analyzing the performance of multilayer piezoelectric transformers”, Proceedings. 1999 IEEE Ultrasonics Symposium, 1999, Volume: 2, pp. 943~946, 1999

[63] De Vries, J.W.C.; Jedeloo, P.; Porath, R.; “Co-fired piezoelectric multilayer transformers”, Proceedings of ISAF '96, Volume: 1, pp. 173~176, 1996

[64] H.Tsuchiya, T. Fukami, “Design Principles for Multiplayer Piezoelectric Transformers”, Ferroelectrics, Vol. 68, pp. 225~234, 1986.

[65] H.Tsuchiya, T. Fukami, "Multiplayered Piezoelectric Transformer", Ferroelectrics, Vol. 63, pp. 299~308, 1985.

[66] D. J. Powell, J. Mould, and G. L. Wojcik, "Dielectric and Mechanical Absorption Mechanisms for Time and Frequency Domain Transducer Modeling", 1998 IEEE Ultrasonic Symposium Proceedings.

[67] S. Hirose, M. Aoyagi, Y. Tomikawa, "Dielectric loss in a piezoelectric ceramic transducer under high-power operation; Increase of dielectric loss and its influence on transducer efficiency," Jpn. J. Appl. Phys., Vol. 32, pp. 2418-2421, 1993.

[68] P. Gonnard and R. Briot, "Studies on dielectric and mechanical properties of PZT doped ceramics, using a model of losses," Ferroelectrics, pp. 580-583, 1991.

[69] R. Briot, P. Gonnard and, M. Troccaz, "Modelization of the Dielectric and Mechanical Losses in Ferroelectric Ceramics," Ferroelectrics, Vol. 93, 1989, pp. 117~126.

[70] J.L. San Emeterio Prieto, F. Montero De Espinosa, et al, "On the Measurement of the Mechanical Loss of Low Qm Piezoelectric Materials", Ferroelectrics, 1988, Vol. 81, pp. 257~260.

[71] Fred C. Lee, "Advanced Power Conversion Techniques—Resonant Power Converter", Class Notes for ECE5244, CPES, Virginia Tech.

[72] C. Y. Lin, "Design and Analysis of Piezoelectric Transformer Converters," Ph.D. Dissertation, Virginia Tech, July 1997.

[73] Eric. M. Baker, Weixing Huang, Dan Y. Chen and Fred C. Lee, "Radial Mode Piezoelectric Transformer Design for Fluorescent Lamp Ballast Applications", 2001 CPES Seminar, pp. 105~112.

[74] J. Qian, "Advanced Single-Stage Power Factor Correction Techniques", Ph.D. Dissertation, Virginia Tech, Sept. 1997

[75] "APC 841-Lead Zirconate Titanate," http://www.americanpiezo.com,

[76] T. Zaitsu, "Power Conversion Using Piezoelectric Transformer," Ph.D. Dissertation, Kyushu University, Fukuoka, Japan, August 1997.

[77] Eric. M. Baker, Weixing Huang, Dan Y. Chen and Fred C. Lee, "Radial Mode Piezoelectric Transformer Design for Fluorescent Lamp Ballast Applications", IEEE PESC'02, pp. 1289~1294

[78] Weixing Huang, Dan Y. Chen, Eric M. Baker, Jinghai Zhou and Fred C. Lee, "Design of a Piezoelectric Transformer for PFC Electronic Ballast", 2002 CPES Seminar, pp. 224~230.

[79] Eric M. Baker, Weixing Huang, Dan Y. Chen and Fred C. Lee, "A Novel Thermally Conductive Mounting Technique for Piezoelectric Transformer", 2002 CPES Seminar, pp. 231~233.

[80] Weiping Zhang, Weixing Huang, Dan Y. Chen and Fred C. Lee, "Characterization of Nonlinear Internal Resistance of a Power Piezoelectric Transformer", 2002 CPES Seminar, pp. 234~236.

[81] D.K. Lindner, M. Zhu, C. Song, W. Huang, D. Cheng, "Low-input voltage switching Amplifier for Piezoelectric Actuator", Proceedings of SPIE'02, SPIE 9th international Conference on Smart Structures and Materials, March, 2002.

[82] Ray-Lee Lin, Fred C. Lee, Eric M. Baker, Dan Y. Chen, “Inductor-less piezoelectric transformer electronic ballast for linear fluorescent lamp”, 2000 CPES Seminar, pp. 309~314.

[83] Ray L. Lin, Eric Baker, and Fred C. Lee, “Characterization of Piezoelectric Transformers,” 1999 VPEC Seminar, pp.219-225.

[84] Ray L. Lin, Pit-Leong Wong, and Fred C. Lee, “An Equivalent Circuit Model of Radial Vibration Mode Piezoelectric Transformers,” 1999 VPEC Seminar at Virginia Tech, pp.120-125.

APPENDIX A. MATHCAD PROGRAM TO ANALYSIS PT

Parameters of AJ-1

$R := 11.1795$ $L := 9.5050310^{-3}$ $C := 192.3610^{-12}$ $N := 0.969466$ $Cd1 := 1.4690510^{-9}$ $Cd2 := 1.3471410^{-9}$

Normalized input voltage $Vin := 1$

Define the load range

$RLmin := 10^{0}$ $RLmax := 10^{6}$ $npts := 1000$ $n := 0..\ npts$ $RL_n := 10^{\frac{\log(RLmax)}{npts}\cdot n}$

Resonance frequency for a given load

$$f_n := \frac{\sqrt{2\cdot C\cdot L\cdot\left[-C\cdot L\cdot N^2 + N^2\cdot Cd2^2\cdot(RL_n)^2 + C\cdot Cd2\cdot(RL_n)^2 + \sqrt{C^2\cdot L^2\cdot N^4 + 2\cdot C\cdot L\cdot N^4\cdot Cd2^2\cdot(RL_n)^2 - 2\cdot C^2\cdot L\cdot N^2\cdot Cd2\cdot(RL_n)^2 + N^4\cdot Cd2^4\cdot(RL_n)^4 + 2\cdot N^2\cdot Cd2^3\cdot(RL_n)^4\cdot C + C^2\cdot Cd2^2\cdot(RL_n)^4}\right]}}{\left(4\cdot\pi\cdot C\cdot L\cdot N\cdot Cd2\cdot RL_n\right)}$$

Voltage gain at the resonance (dB)

$$A_n := 20\cdot\log\left[\frac{RL_n}{\left[N^2\cdot R\cdot\left[1+\left(2\cdot\pi\cdot f_n\right)^2\cdot(RL_n)^2\cdot Cd2^2\right]\right]+RL_n}\cdot\sqrt{1+\left(2\cdot\pi\cdot f_n\right)^2\cdot(RL_n)^2\cdot Cd2^2}\right]$$

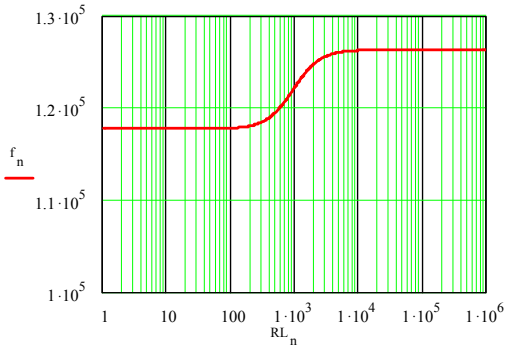

Normalized Output Power at Resonance

$$Po_n := Vin^2\cdot\frac{N^2\cdot RL_n\cdot\left[1+\left(2\cdot\pi\cdot f_n\right)^2\cdot(RL_n)^2\cdot Cd2^2\right]}{\left[\left[N^2\cdot R\cdot\left[1+\left(2\cdot\pi\cdot f_n\right)^2\cdot(RL_n)^2\cdot Cd2^2\right]\right]+RL_n\right]^2}$$

Efficiency at Resonance

$$\eta_n := \frac{1}{1+\left[1+\left(2\cdot\pi\cdot f_n\right)^2\cdot(RL_n)^2\cdot Cd2^2\right]\frac{N^2\cdot R}{RL_n}}$$

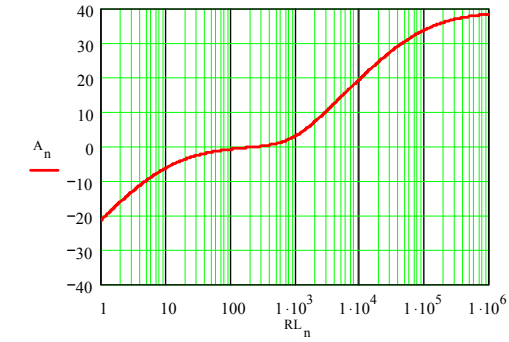

Definitions for the Normalization

$k := \frac{N^2\cdot Cd2}{C}$ $\omega 0 := \frac{1}{\sqrt{L\cdot C}}$ $Z0 := \sqrt{\frac{L}{C}}$ $Qm := \frac{Z0}{R}$

Define the range of the Normalized frequency

$fn := 0, 0.001.. 2$

Voltage Gain in dB

$$Av(fn, RL) := 20\cdot\log\left[\frac{1}{\sqrt{\left[1+\frac{\frac{N^2\cdot Z0}{RL}}{Qm}+k\cdot\left(1-fn^2\right)\right]^2+\left[fn\cdot\frac{k}{Qm}+\frac{1}{fn}\cdot\frac{N^2\cdot Z0}{RL}\cdot\left(fn^2-1\right)\right]^2}}\right]$$

3D analysis of the Simplified Equivalent Circuit Model for PTs

Set the working frequency range:

$f_{min} := 50000 \qquad f_{max} := 150000 \qquad npts := 100 \qquad n := 0 .. npts$

$f_n := f_{min} + \frac{(f_{max} - f_{min})}{npts} \cdot n$

Set the Load Range:

$RL_{min} := 1 \qquad RL_{max} := 1000 \qquad mpts := 50 \qquad m := 0 .. mpts$

$RL_m := RL_{min} + \frac{(RL_{max} - RL_{min})}{mpts} \cdot m$

$CF := 5 \qquad tan\delta := 0.005 \qquad tan\delta := CF \cdot tan\delta$

CF is the Correction factor for the material dissipation loss due to the specification being given at 1kHz

Dielectric loss

$Rcd1_n := \frac{1}{2\pi \cdot f_n \cdot tan\delta \cdot Cd1} \qquad Rcd2_n := \frac{1}{2\pi \cdot f_n \cdot tan\delta \cdot Cd2}$

Voltage Gain as a function of RL and fs, Considering the dielectric loss

$$Av\_esr_{m,n} := \left| N \frac{\frac{\frac{RL_m}{N^2} \frac{1}{\left(\frac{N^2}{Rcd2_n} + 2\cdot\pi\cdot i\cdot f_n \cdot N^2 \cdot Cd2\right)}}{\frac{RL_m}{N^2} + \frac{1}{\left(\frac{N^2}{Rcd2_n} + 2\cdot\pi\cdot i\cdot f_n \cdot N^2 \cdot Cd2\right)}}}{R + 2\cdot\pi\cdot i\cdot f_n \cdot L + \frac{1}{2\cdot\pi\cdot i\cdot f_n \cdot C} + \frac{\frac{\frac{RL_m}{N^2} \frac{1}{\left(\frac{N^2}{Rcd2_n} + 2\cdot\pi\cdot i\cdot f_n \cdot N^2 \cdot Cd2\right)}}{\frac{RL_m}{N^2} + \frac{1}{\left(\frac{N^2}{Rcd2_n} + 2\cdot\pi\cdot i\cdot f_n \cdot N^2 \cdot Cd2\right)}}}{\frac{RL_m}{N^2} + \frac{1}{\left(\frac{N^2}{Rcd2_n} + 2\cdot\pi\cdot i\cdot f_n \cdot N^2 \cdot Cd2\right)}}} \right|$$

Voltage Gain as a function of RL and fs without considering the dielectric loss

$$Av_{m,n} := \left| N \frac{\frac{\frac{RL_m}{N^2} \frac{1}{2\cdot\pi\cdot i\cdot f_n \cdot N^2 \cdot Cd2}}{\frac{RL_m}{N^2} + \frac{1}{2\cdot\pi\cdot i\cdot f_n \cdot N^2 \cdot Cd2}}}{R + 2\cdot\pi\cdot i\cdot f_n \cdot L + \frac{1}{2\cdot\pi\cdot i\cdot f_n \cdot C} + \frac{\frac{\frac{RL_m}{N^2} \frac{1}{2\cdot\pi\cdot i\cdot f_n \cdot N^2 \cdot Cd2}}{\frac{RL_m}{N^2} + \frac{1}{2\cdot\pi\cdot i\cdot f_n \cdot N^2 \cdot Cd2}}}{\frac{RL_m}{N^2} + \frac{1}{2\cdot\pi\cdot i\cdot f_n \cdot N^2 \cdot Cd2}}} \right|$$

Input Impedance with considering of the dielectric loss

$$Zin\_esr_{m,n} := \frac{\frac{1}{\left(\frac{1}{Rcd1_n} + 2\cdot\pi\cdot i\cdot f_n\cdot Cd1\right)}\cdot\left[R + \frac{1}{2\cdot\pi\cdot i\cdot f_n\cdot C} + 2\cdot\pi\cdot i\cdot f_n\cdot L + \frac{\frac{RL_m}{N^2}\cdot\left(\frac{N^2}{Rcd2_n} + 2\cdot\pi\cdot i\cdot f_n\cdot N^2\cdot Cd2\right)^{-1}}{\frac{RL_m}{N^2} + \left(\frac{N^2}{Rcd2_n} + 2\cdot\pi\cdot i\cdot f_n\cdot N^2\cdot Cd2\right)^{-1}}\right]}{\frac{1}{\left(\frac{1}{Rcd1_n} + 2\cdot\pi\cdot i\cdot f_n\cdot Cd1\right)} + \left[R + \frac{1}{2\cdot\pi\cdot i\cdot f_n\cdot C} + 2\cdot\pi\cdot i\cdot f_n\cdot L + \frac{\frac{RL_m}{N^2}\cdot\left(\frac{N^2}{Rcd2_n} + 2\cdot\pi\cdot i\cdot f_n\cdot N^2\cdot Cd2\right)^{-1}}{\frac{RL_m}{N^2} + \left(\frac{N^2}{Rcd2_n} + 2\cdot\pi\cdot i\cdot f_n\cdot N^2\cdot Cd2\right)^{-1}}\right]}$$

Input Impedance without considering the dielectric loss

$$Zin_{m,n} := \frac{\frac{1}{\left(2\cdot\pi\cdot i\cdot f_n\cdot Cd1\right)}\cdot\left(R + \frac{1}{2\cdot\pi\cdot i\cdot f_n\cdot C} + 2\cdot\pi\cdot i\cdot f_n\cdot L + \frac{\frac{RL_m}{N^2}\cdot\frac{1}{2\cdot\pi\cdot i\cdot f_n\cdot N^2\cdot Cd2}}{\frac{RL_m}{N^2} + \frac{1}{2\cdot\pi\cdot i\cdot f_n\cdot N^2\cdot Cd2}}\right)}{\frac{1}{\left(2\cdot\pi\cdot i\cdot f_n\cdot Cd1\right)} + \left(R + \frac{1}{2\cdot\pi\cdot i\cdot f_n\cdot C} + 2\cdot\pi\cdot i\cdot f_n\cdot L + \frac{\frac{RL_m}{N^2}\cdot\frac{1}{2\cdot\pi\cdot i\cdot f_n\cdot N^2\cdot Cd2}}{\frac{RL_m}{N^2} + \frac{1}{2\cdot\pi\cdot i\cdot f_n\cdot N^2\cdot Cd2}}\right)}$$

Input Power, Output Power and Efficiency with considering dielectric loss

$$Pin\_esr_{m,n} := Re\left(\frac{Vin^2}{Zin\_esr_{m,n}}\right) \qquad Pout\_esr_{m,n} := \frac{\left(Vin\cdot Av\_esr_{m,n}\right)^2}{RL_m} \qquad Eff\_esr_{m,n} := \frac{Pout\_esr_{m,n}}{Pin\_esr_{m,n}}$$

Input Power, Output Power and Efficiency without Considering dielectric loss

$$Pin_{m,n} := Re\left(\frac{Vin^2}{Zin_{m,n}}\right) \qquad Pout_{m,n} := \frac{\left(Vin\cdot Av_{m,n}\right)^2}{RL_m} \qquad Eff_{m,n} := \frac{Pout_{m,n}}{Pin_{m,n}}$$

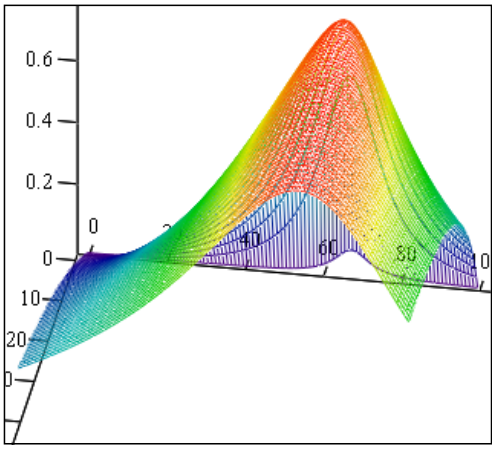

Eff_esr

APPENDIX B. MATHCAD PROGRAM TO DESIGN PT FOR PFC BALLAST

Materials choosen: APC841, the material properties is listed as following:

a) *definitions*

ρ : Material Density
ε : Permittivity of the Material
Qm : Mechanical Quality Factor
d : Piezoelectric Coefficient
S : Elastic Compliance

t1 : Thickness of a Single Primary Layer
t2 : Thickness of a Single Secondary Layer
N1 : Number of Primary Layers
N2 : Number of Secondary Layers

b) *relationship between the PT Equivalent CKT parameter and the material properties*

$$C_{d1} = \frac{N_1 \cdot \pi \cdot r^2 \cdot \varepsilon_{33} \cdot \left(1 - \frac{d_{31}^2}{\varepsilon_{33} \cdot s_{11}}\right)}{t_1} \qquad R = \frac{\sqrt{2 \cdot \rho \cdot s_{11}^3} \cdot (N_1 \cdot t_1 + N_2 \cdot t_2)}{16 \cdot r \cdot Qm \cdot (N \cdot d_{31})^2} \qquad L = \frac{2 \cdot r \cdot \rho \cdot s_{11}^2 \cdot (N_1 \cdot t_1 + N_2 \cdot t_2)}{16 \cdot \pi \cdot r \cdot (N \cdot d_{31})^2}$$

$$C = \frac{16 r^2 \cdot (d_{31} \cdot N)^2}{\pi \cdot s_{11} \cdot (N_1 \cdot t_1 + N_2 \cdot t_2)} \qquad C_{d2} = \frac{N_2 \cdot \pi \cdot r^2 \cdot \varepsilon_{33} \cdot \left(1 - \frac{d_{31}^2}{\varepsilon_{33} \cdot s_{11}}\right)}{t_2} \qquad N = \frac{N_1}{N_2}$$

C) D*esign Process*

AP841 Piezoelectric Ceramic Materials Charateristic

$\varepsilon 0 := 8.854 \cdot 10^{-12} \frac{F}{m}$ $\quad \varepsilon 33 := 1350 \cdot \varepsilon 0$ $\quad Qm := 1400$

$\rho := 7.6 \cdot 10^{-3} \cdot \frac{kg}{cm^3}$ $\quad d31 := -109 \cdot 10^{-12} \cdot \frac{m}{V}$ $\quad S11 := 11.7 \cdot 10^{-12} \cdot \frac{m^2}{N}$

$Np := 2055 \cdot \frac{m}{s}$ $\quad \tan\delta := 0.0035$

Step1 Load Matching

At first the resonant frequency could be initially chosen according to the diameter of the PT, Which is related to the thermal issue.

Select $D := 0.825 \cdot in$

The radius of the PT could be calculated as: $r := \frac{D}{2}$ $\quad r = 0.413\,in$

and the resonant frequecy could be calculated accordingly

$f0 := \frac{Np}{D}$ $\quad f0 = 98.067\,kHz$

The lamp resistance RL is equal to 500ohm, using load matching, we have

$RL := 500 \cdot ohm$

$Cd2 := \frac{1}{2 \cdot \pi \cdot f0 \cdot RL} \qquad Cd2 = 3.246\,nF$

Assume only one layer is utilized for the secondary, then t2 could me calculated as following:

$N2 := 1 \qquad t2 := \frac{N2 \cdot \pi \cdot r^2 \cdot \varepsilon 33 \cdot \left(1 - \frac{d31^2}{\varepsilon 33 \cdot S11}\right)}{Cd2} \qquad t2 = 0.046\,in$

Round t2 to 50 mil, 60mils was selected due to availability $t2 := 0.06 \cdot in$

At first, Let us Choose N1=1 and N2=1, If we can not the required region, we can repeat the process, increasing the layer of N1, When N1=4, a solution can be found

$N1 := 4 \qquad N2 := 1 \qquad N := \frac{N1}{N2}$

Choose a range of t1, 10mil-200mil

$t1_{min} := 0.01in \qquad t1_{max} := 0.20in \qquad npts := 100 \qquad n := 0 .. npts$

$t1_n := t1_{min} + \frac{\left(t1_{max} - t1_{min}\right)}{npts} \cdot n$

Set the frequency range

$f_{min} := 90kHz \qquad f_{max} := 130kHz \qquad mpts := 100 \qquad m := 0 .. mpts$

$f_m := f_{min} + \frac{\left(f_{max} - f_{min}\right)}{mpts} \cdot m$

then the parameters in the equivalent CKT are the function of t1

$Cd1_n := \frac{N1 \cdot \pi \cdot r^2 \cdot \varepsilon 33 \cdot \left(1 - \frac{d31^2}{\varepsilon 33 \cdot S11}\right)}{t1_n} \qquad R_n := \frac{\sqrt{2 \cdot \rho \cdot S11^3} \cdot \left(N1 \cdot t1_n + N2 \cdot t2\right)}{16 \cdot r \cdot Qm \cdot (N1 \cdot d31)^2}$

$L_n := \frac{2 \cdot r \cdot \rho \cdot S11^2 \cdot \left(N1 \cdot t1_n + N2 \cdot t2\right)}{16 \cdot \pi \cdot r \cdot (N1 \cdot d31)^2} \qquad C_n := \frac{16 \cdot r^2 \cdot (N1 \cdot d31)^2}{\pi \cdot S11 \cdot \left(N1 \cdot t1_n + N2 \cdot t2\right)}$

If taking the dielectric loss into account and select the correct factor as

$CF := 1 \qquad tan\delta := tan\delta \cdot CF$

$Rcd1_{m,n} := \frac{1}{2\pi \cdot f_m \cdot tan\delta \cdot Cd1_n} \qquad Rcd2_m := \frac{1}{2\pi \cdot f_m \cdot tan\delta \cdot Cd2}$

STEP2 Voltage Gain Critiral

The RMS value of the line voltage is $Vac := 120V$

So the peak value of the line input voltage is $Vac\_peak := \sqrt{2}\,Vac$

The Rectified DC Bus Voltage is around: $Vbus := 155V$

The Power of the Lamp is 32W $Pout := 32W$

Since the input voltage of the piezoelectric transformer is a trapezoidal waveform, considering the fundamental driving frequency, the peak value of the PT input voltage is

$$Vin\_peak := \frac{2}{\pi}\cdot\frac{\sin(\pi\cdot 0.25)}{\pi\cdot 0.25}\cdot Vbus$$

So the RMS value of the PT input voltage is

$$Vin\_rms := \frac{Vin\_peak}{\sqrt{2}}$$

Then the required voltage should be

$$Av_{min} := \frac{\sqrt{Pout\cdot RL}}{Vin\_rms} \qquad Av_{min} = 2.014$$

Voltage gain of the PT could be calculated as:

$$Av_{m,n} := \left| N\cdot\frac{\frac{\frac{RL}{N^2}}{\left(\frac{N^2}{Rcd2_m}+2\cdot\pi\cdot i\cdot f_m\cdot N^2\cdot Cd2\right)}}{\frac{RL}{N^2}+\frac{1}{\left(\frac{N^2}{Rcd2_m}+2\cdot\pi\cdot i\cdot f_m\cdot N^2\cdot Cd2\right)}}}{R_n+2\cdot\pi\cdot i\cdot f_m\cdot L_n+\frac{1}{2\cdot\pi\cdot i\cdot f_m\cdot C_n}+\frac{\frac{RL}{N^2}\cdot\frac{1}{\left(\frac{N^2}{Rcd2_m}+2\cdot\pi\cdot i\cdot f_m\cdot N^2\cdot Cd2\right)}}{\frac{RL}{N^2}+\frac{1}{\left(\frac{N^2}{Rcd2_m}+2\cdot\pi\cdot i\cdot f_m\cdot N^2\cdot Cd2\right)}}}\right|$$

To meet the volage again requirement, we need

$$SOL1_{m,n} := \begin{cases} 1 & \text{if } Av_{m,n} > Av_{min} \\ 0 & \text{otherwise} \end{cases}$$

STEP3 ZVS Critiral

$$Z3_m := \frac{\frac{RL}{N^2}\cdot\frac{1}{\left(\frac{N^2}{Rcd2_m} + 2\cdot\pi\cdot i\cdot f_m\cdot N^2\cdot Cd2\right)}}{\frac{RL}{N^2} + \frac{1}{\left(\frac{N^2}{Rcd2_m} + 2\cdot\pi\cdot i\cdot f_m\cdot N^2\cdot Cd2\right)}} \qquad Z2_{m,n} := R_n + i\cdot 2\cdot\pi\cdot f_m\cdot L_n + \frac{1}{i\cdot 2\cdot\pi\cdot f_m\cdot C_n}$$

$$Z1_{m,n} := Z2_{m,n} + Z3_m$$

$$\Delta i_{L_{m,n}} := \frac{Vbus\cdot\frac{2}{\pi}}{\left|Z1_{m,n}\right|}\cdot\left[\left(\frac{\sin(\pi\cdot 0.25)}{\pi\cdot 0.25}\right)^1\cdot\sin\left(\arg\left(Z1_{m,n}\right)\right)\right]$$

$$\Delta i_{Lcritical_n} := \sqrt{\frac{Cd1_n\cdot\left(C_n + Cd1_n\right)}{L_n\cdot C_n}}\cdot Vbus$$

To meet the ZVS requirement, we need:

$$SOL2_{m,n} := \begin{cases} 1 & \text{if } \Delta i_{L_{m,n}} > \Delta i_{Lcritical_n} \\ 0 & \text{otherwise} \end{cases}$$

STEP4 Efficiency Requirements

The input impedance is

$$Zin_{m,n} := \frac{\frac{1}{\frac{1}{Rcd1_{m,n}} + 2\cdot\pi\cdot i\cdot f_m\cdot Cd1_n}\cdot Z1_{m,n}}{\frac{1}{\frac{1}{Rcd1_{m,n}} + 2\cdot\pi\cdot i\cdot f_m\cdot Cd1_n} + Z1_{m,n}}$$

Input Power is

$$Pin_{m,n} := Re\left[\frac{(Vin\_rms)^2}{Zin_{m,n}}\right]$$

Output power is

$$Pout_{m,n} := \frac{\left(Vin\_rms\cdot Av_{m,n}\right)^2}{RL}$$

Efficiency

$$Eff_{m,n} := \frac{Pout_{m,n}}{Pin_{m,n}}$$

If we need the min efficiency of the PT is above 90%, set $Eff_{min} := 0.9$

$$SOL3_{m,n} := \begin{cases} 1 & \text{if } Eff_{m,n} > Eff_{min} \\ 0 & \text{otherwise} \end{cases}$$

STEP5 PFC Requirement

$$I_{L_{m,n}} := \frac{Vin\_peak}{|Z1_{m,n}|} \qquad I_{PFC_{m,n}} := \pi \cdot \left[\frac{2 \cdot Pout_{m,n}}{Eff_{m,n} \cdot f_m \cdot (Vac\_peak)^2} + Cd1_n \right] \cdot f_m \cdot Vbus$$

$$SOL4_{m,n} := \begin{cases} 1 & \text{if } I_{L_{m,n}} \geq I_{PFC_{m,n}} \\ 0 & \text{otherwise} \end{cases}$$

STEP6 Overall Evaluation

$$SOL_{m,n} := \begin{cases} 1 & \text{if } SOL1_{m,n} \cdot SOL2_{m,n} \cdot SOL3_{m,n} \cdot SOL4_{m,n} = 1 \\ 0 & \text{otherwise} \end{cases}$$

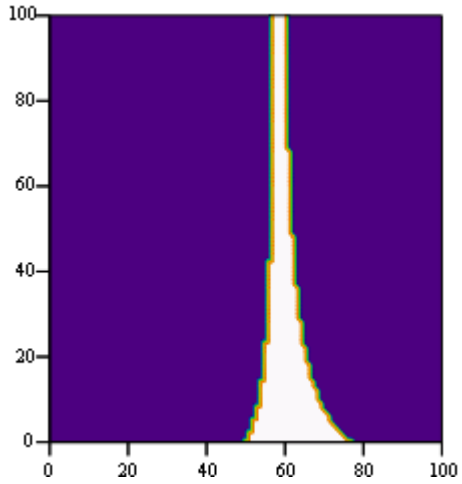

SOL1

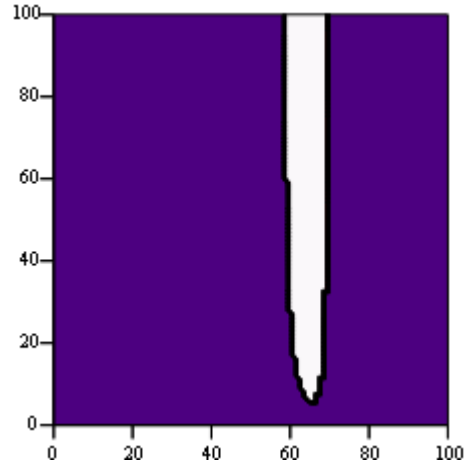

SOL2

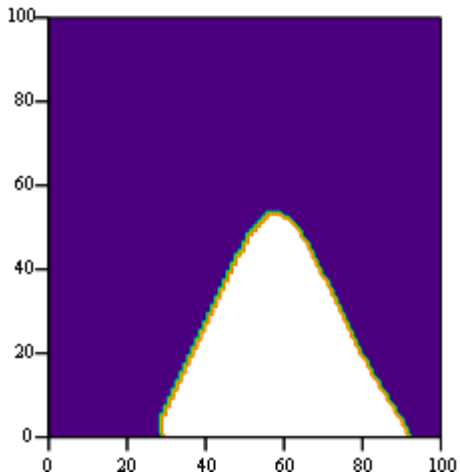

SOL3

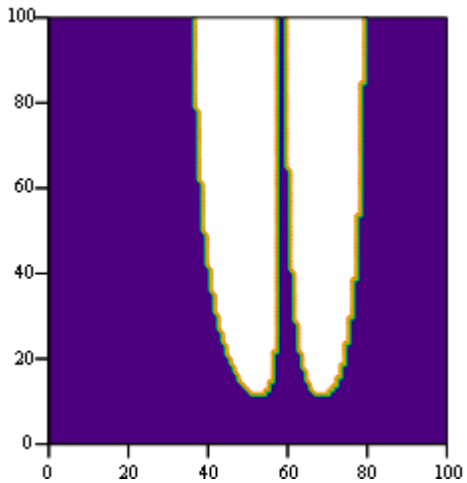

SOL4

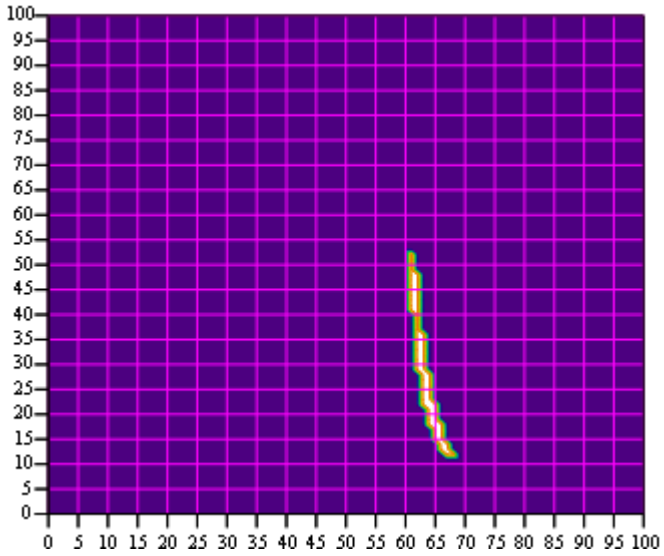

SOL

Now we can get one possibe design from the above region and evaluate the characterisitic of the new designed PT. Data and parameters are listed below for summary. Note (1) t1 is selected according the availability of the materials. Here t1=60mils; (2) In the above plot the axis nubmer are not the actual number but subscript of t1. for example, $t1_{26}$ is actually 59mil. (3)To draw the plot with acutal number as the axis, we can export the data to excel and generate the curve as shown in the thesis.

The thickness of t1 selected as $t1_{26} = 0.059\,\text{in}$

and the related frequency is $f_{63} = 115.2\,\text{kHz}$

Summery for the designed PT

Dimensional parameters

$t1 := 0.06\cdot\text{in}$ $t2 := 0.06\text{in}$ $r := 0.4125\text{in}$ $D := 2\cdot r$ $D = 0.825\,\text{in}$

$N1 := 4$ $N2 := 1$

Using the characteristic equations to get the equivalent circuit parameters

$$Cd1 := \frac{N1\cdot\pi\cdot r^2\cdot\varepsilon 33\cdot\left(1-\frac{d31^2}{\varepsilon 33\cdot S11}\right)}{t1} \qquad R := \frac{\sqrt{2\cdot\rho\cdot S11^3}\cdot(N1\cdot t1 + N2\cdot t2)}{16\cdot r\cdot Qm\cdot(N1\cdot d31)^2} \qquad L := \frac{2\cdot r\cdot\rho\cdot S11^2\cdot(N1\cdot t1 + N2\cdot t2)}{16\cdot\pi\cdot r\cdot(N1\cdot d31)^2}$$

$$C := \frac{16\cdot r^2\cdot(N1\cdot d31)^2}{\pi\cdot S11\cdot(N1\cdot t1 + N2\cdot t2)} \qquad Cd2 := \frac{N2\cdot\pi\cdot r^2\cdot\varepsilon 33\cdot\left(1-\frac{d31^2}{\varepsilon 33\cdot S11}\right)}{t2} \qquad N := \frac{N1}{N2}$$

Equivalent circuit parameters:

$Cd1 = 9.9\times10^{-9}\,\text{F}$ $R = 0.843\,\Omega$ $L = 1.659\times10^{-3}\,\text{H}$ $C = 1.192\times10^{-9}\,\text{F}$

$Cd2 = 2.475\times10^{-9}\,\text{F}$ $N = 4$

VITA

The author was born in Wuhan, Hubei province, P. R. China, in 1976. He received his B.S. degree and M.S. degrees both in Electrical Engineering from Huazhong University of Science and Technology (HUST), Wuhan, P. R. China in 1997 and 2000, respectively.

From 1997 to 2000, the author worked as a Research Assistant in the National Specialized Laboratory of New Type Electrical Machinery at the Department of Electrical Engineering of HUST, focusing on electric machine and motor drives.

Since August 2000, he has been with the Center for Power Electronics System (CPES) at Virginia Polytechnic Institute and State University, Concentrating on the study and research of power electronics. His research focused on the design of piezoelectric transformer and associated power electronic circuits.